Renewable Energy Penetration Planning

For Remote Power Grid

by

Yujia Zhu

A Thesis Presented in Partial Fulfillment
of the Requirements for the Degree
Master of Science

Approved July 2012 by the
Graduate Supervisory Committee

Keith Holbert, Chair
George Karady
Daniel Tylavsky

ARIZONA STATE UNIVERSITY

August 2012

ABSTRACT

Power generation in remote isolated places is a tough problem. Presently, a common source for remote generation is diesel. However, diesel generation is costly and environmental unfriendly. It is promising to replace the diesel generation with some clean and economical generation sources.

The concept of renewable generation offers a solution to remote generation. This thesis focuses on evaluation of renewable generation penetration in the remote isolated grid. A small town named Coober Pedy in South Australia is set as an example. The first task is to build the stochastic models of solar irradiation and wind speed based on the local historical data. With the stochastic models, generation fluctuations and generation planning are further discussed. Fluctuation analysis gives an evaluation of storage unit size and costs. Generation planning aims at finding the relationships between penetration level and costs under constraint of energy sufficiency. The results of this study provide the best penetration level that makes the minimum energy costs. In the case of Coober Pedy, cases of wind and photovoltaic penetrations are studied. The additional renewable sources and suspended diesel generation change the electricity costs. Results show that in remote isolated grid, compared to diesel generation, renewable generation can lower the energy costs.

AKNOWLEDGEMENT

I would like to give my sincere thanks to my advisor, Dr. Keith Holbert, whose advice has guided me from topic selection to the final level. It is also my great honor to have Dr. George Karady and Dr. Daniel Tylavsky in my supervisory committee and thanks for their time and guidance. I owe my gratitude to all faculties in group of power system engineering. They lead me to the path to enter the field of power system engineering and finish this thesis.

Words can’t describe my admiration and affection to my family for raising me and supporting me continuously. Finally, thanks to all my friends, without whom, I may not make this thesis realized.

TABLE OF CONTENTS

Page

LIST OF TABLES

TABLE Page

LIST OF FIGURES

FIGURE Page

1. Introduction

1.1 Background

Historically, a long term challenge for the power system engineer is to supply sufficient and high quality energy to satisfy the growing demands. To deal with the challenge, a great amount of research has been done.

Remote isolated grids are small-scaled grids in places far from the bulk power grid. Unlike bulk grids, remote isolated power grids are usually on kilowatt bases [1]. For most of the remote grids, the generation or load levels are around or not higher than 1 MW and the load profiles are mainly made up by the residential loads. As a result, the problem of remote generation is not the complex network of the large grid but how to generate sufficient power and make the remote places electrified.

Unlike places within the main power grid, most of the remote areas, like islands and mountainous regions, are off-grid. To provide the power for such places, two solution options may be given: extend to the grid or use local power generation.

The first solution always confronts a dilemma: paying high capital costs for the long distance transmission infrastructure to support low demand at the remote areas [1][2]. Besides the economical problem, long distance grid connection will also face technical problems: power losses within long transmission and the thermal limit of the transmission lines. Compared to grid connection, islanded generation will avoid the problems of building transmission

lines. In some places building local independent power plants is more economical than grid connection [1]-[4].

Currently, remote generations are mainly supported by diesel generators. Advantages of diesel generators are flexibility, reliability and high capacity factors (about 90%) [5] (without backup power). However, disadvantages of diesel generators are obvious. Environmental problem and the health hazard are reported in [6]. More significant, cost of diesel generation is prohibitive. Reference [7] shows the cost of diesel fuel has been more than doubled in the last decade see Fig. 1-1.

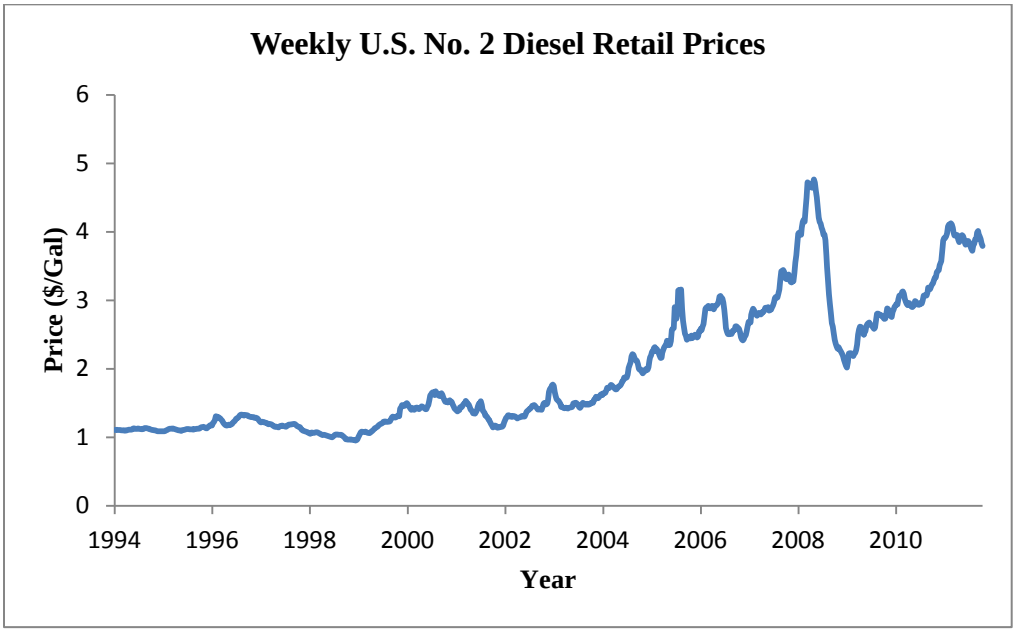

Fig. 1-1 Retail diesel price from 1994-2011.

The development of renewable energy endows a promising future for remote generation. Unlike conventional generators, renewable generation almost take all their ‘fuel’ from nature like wind or solar. Consequently the growing fossil fuel costs will not affect renewable generations. The advantage of renewable

generations is decent. But the renewable sources require comparatively large areas or spaces to make utility size generation. This may be a problem for some urban center areas like cities but not for remote areas.

1.2 Scope of the study

The scope of this study is to model and analyze renewable energy penetration within Coober Pedy, Australia. Detailed models of renewable energy device or control systems are not considered. There are some researches and implementations done in some isolated grids [9][10]. Results of these researches show that in remote areas like Pacific islands, villages in India, towns in the state of Alaska, etc, renewable sources are abundant and good substitutes for diesel to solve the problem of energy insufficiency.

In [1], 250 kW of wind generation is suggested by the local government of Coober Pedy. The present study will analyze the model of renewable energy for Coober Pedy and find out the relationship between penetration level and energy costs. The results of this study will be compared to the government's report.

1.3 Organization of the thesis

The thesis is divided into five chapters. In Chapter 1, a brief introduction of the study is given. In Chapter 2, the background of the study is introduced and problems to be solved are discussed. In Chapter 3, stochastic models of wind speed and solar radiation levels are modeled and tested. In Chapter 4, generation fluctuations of renewable sources are discussed and the size of storage units are calculated. In Chapter 5, planning of the renewable generation in Coober Pedy is

studied. Two factors are considered: costs of energy and generation sufficiency. Chapter 6 concludes.

2. Background

A number of projects about remote renewable penetration are introduced in [1][8]-[13]. In [8], cases of renewable generation for the island of Maldive and a village of India are introduced. Report [13] shows in an island of Maldive with wind generation penetrated into original diesel generation grid, the original energy cost is lowered from 51 cents to 43 cents. For the case in Alaska [11] shows with 51% penetration of wind generation, the Net Present Costs (NPC) can be lowered by 10% and the greenhouse emission can be lowered by 37%. A proposal of integrating renewable sources into the grid of northern Ontario in Canada [12], without quantitative results, estimates that renewable energy will help solve the urgent need of reducing energy costs and pollutions from fossil fuel generation.

2.1 Location of interest

A remote grid of Coober Pedy is studied in this research. Coober Pedy is a town located is South Australia (29^{o} S, 135^{o} E), see Fig. 2-1. The climate of Coober Pedy is semi-desert: very little rainfall but strong wind and sunshine. The current power source of Coober Pedy is 100% diesel. The abundant renewable sources offer a good potential to replace the diesel generators. This study will focus on costs and energy sufficiency of this replacement.

Fig. 2-1 Location of Coober Pedy.

Coober Pedy is a tourism resort. The load in Coober Pedy is composed by residential loads. The peak high load level occurs in summer, when the temperature is high.

Load and generation in Coober Pedy are assumed to be separately centralized in one spot. Hence, the grid network in Coober Pedy is a 'one-wire' model; see Fig. 2-2.

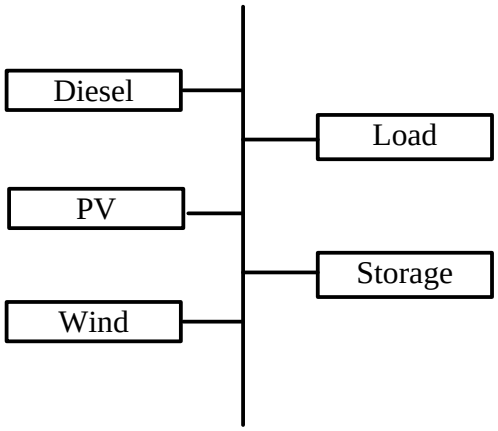

Fig. 2-2 Model of Coober Pedy power grid.

The results of the study will not only illustrate the situation of Coober Pedy. More important, for most of the remote grids that purely depend on diesel generations, Coober Pedy can be a representative, the costs and reliability assessment introduced in this study will share some clues for future researches.

2.2 Problems in renewable energy generation

Two main problems are involved in renewable energy planning: modeling and planning. Modeling will build up the model that fixes the local renewable source pattern and make up the correct estimation of output power. Planning will focus on costs and reliability of the generation.

2.2.1 Wind output power modeling

The typical relationship between wind speed and wind power can be described by a cubic function [14]:

$$P_w = \frac{1}{2}\rho A v^3 \tag{2-1}$$

where, P_w is the wind power; A is the swept area in m^2; ρ is the air density; and v is the wind speed. Wind turbines cannot fully convert the wind power, the maximum efficiency, namely Betz optimum efficiency, is 59.3% [15]. Parameters of wind turbines further limit the efficiency. To accurately calculate the wind turbine output, another set of equations describe the relationship between wind speed and wind turbine output power [16]:

$$P_w = \begin{cases} 0 & 0 \le SW_t < V_{ci} \\ (A + B \times SW_t + C \times SW_t^2) \times P_r & V_{ci} \le SW_t < V_r \\ P_r & V_r \le SW_t < V_{co} \\ 0 & SW_t \ge V_{co} \end{cases} \quad (2\text{-}2)$$

where,

$$A = \frac{1}{(V_{ci} - V_r)^2} \left[V_{ci}(V_{ci} + V_r)] - 4V_{ci}V_r \frac{(V_{ci} - V_r)^3}{2V_r} \right]$$

$$B = \frac{1}{(V_{ci} - V_r)^2} \left[4(V_{ci} + V_r) \frac{(V_{ci} + V_r)^3}{2V_r} - (3V_{ci} + V_r) \right]$$

$$C = \frac{1}{(V_{ci} - V_r)^2} \left[2 - 4 \frac{(4V_{ci} + V_r)^3}{2V_r} \right]$$

V_{ci}, V_{co}, V_r are cut in speed, cut out speed and rated speed respectively; SW is the given wind speed; and P_r is rated output power, see Fig. 2-3.

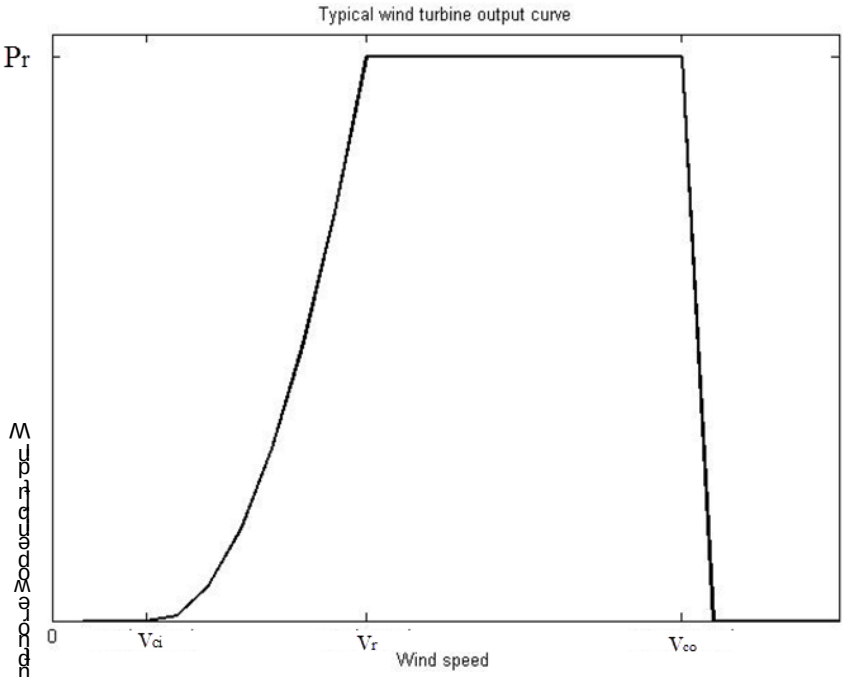

Fig. 2-3 Wind turbine output and wind speed.

2.2.2 PV output power modeling

Output energy of the PV panel needs carefully calculation. Two kinds of simulation or calculation methods are introduced by researchers. The first method calculates the output power based on the model of the panel [17]. In [17] output voltage and current are calculated based on the radiance level and temperature of the panel. This method can be used to perform time sequential simulation. In [18], an equation, which considers the solar angles, is given:

$$P_{pv} = R A_p \eta_p \tag{2-3}$$

where R is the total irradiation on the panel; A is panel area; η_p is the efficiency of Maximum Power Point Tracking (MPPT). The total irradiation on the panel is a value that involves solar angle and panel angles. The calculation of solar angles for Coober Pedy will be discussed in Chapter 5.

2.2.3 Stochastic modeling of renewable sources

It is shown in Equations (2-2) and (2-3), there are two variables whose values are given by nature: wind speed and solar irradiation. Unlike conventional fuel which can be determined and estimated by people, natural ‘fuels’ are intermittent and unpredictable. Hence stochastic models are needed to describe the renewable sources models.

Using a distribution function to establish renewable source histograms is a quick approach to build up the model. For solar irradiation and wind speed, there are four common distribution functions: the Weibull distribution, the beta distribution, the normal distribution and the exponential distribution.

The most commonly used model of renewable sources is the Weibull probability density function (PDF) [19]-[22]. The Weibull PDF is a two-parameter distribution function shown in (2-4). The detailed description of the Weibull PDF is given in [21]. To determine parameters a and b, three methods are used in reference [19] and the maximum likelihood method turns out to be the best approach.

$$f(x,a,b)=\frac{b}{a}\left(\frac{x}{a}\right)^{b-1}e^{-(x/a)^b} \tag{2-4}$$

In the equation parameters x is the random variable. a and b are the two factors that describe the shape of the distribution: a is the scaling factor and b is the shape factor.

The normal distribution PDF is used by [23][24]. Reference [23] points out that in case of lacking sufficient historical data, the Weibull distribution is more complicated to build than the normal distribution. To make the modeling more practical, references [23][24] propose a general model with normal distribution. This general model needs data of local climate pattern.

The beta distribution function is used to model solar distribution in [17]. A drawback of the beta distribution function is that it requires that the data are all in range between 0 and 1 which will require converting the data and may generate some errors.

$$f_s(s)=\begin{cases}\dfrac{\Gamma(\alpha+\beta)}{\Gamma(\alpha)\Gamma(\beta)}s^{(\alpha-1)}\\ 0\end{cases} \tag{2-5}$$
$$s.t.\ 0\le s\le 1,\alpha\ge 0$$

where s denote solar radiance, α and β denote parameters of beta function which can be calculated by

$$\begin{aligned} \beta &= (1-\mu)\left(\frac{\mu(1+\mu)}{\sigma^2}-1\right) \\ \alpha &= \frac{\mu\beta}{1-\mu} \end{aligned} \tag{2-6}$$

where μ is the mean value of the data and σ is the standard deviation.

The exponential distribution can be described by:

$$f(x,\lambda) = \lambda e^{-\lambda x} \tag{2-7}$$

where x is the random variable and λ is the function parameter namely rate parameter.

Random process is another method to build a wind model. Auto Regressive and Moving Average (ARMA) time series modeling is commonly used [23]-[26]. This method can reveal the correlation of wind speed between different time spots; however, it may ignore some extreme cases like sudden change of wind speed. A typical ARMA model can be described by:

$$y_t = a_1 y_{t-1} + a_2 y_{t-2} + \cdots + a_n y_{t-n} + \varepsilon_t + \varepsilon_{t-1} b_1 + \cdots \varepsilon_{t-m} b_m \tag{2-8}$$

where y_i denotes the wind speed at any time and ε_j is the normal white noise with zero mean and variance σ^2. The parameters a_i and b_j are calculated by nonlinear least square method in [23][24].

2.2.4 Testing goodness of fit

When the stochastic model is built, it is necessary to test the model and determine whether it can fit the original histogram. The Kolmogorov–Smirnov test (K-S test) is used in this study.

The K-S test is a nonparametric test for the quality of continuous, one-dimensional probability distributions that can be used to compare a sample with a reference probability distribution, or to compare two samples. In (2-9), $F_n(x)$ calculates the probability that the variable X lies in the section that $X \le x$, where n is the number of data and $I_{X_i \le x}$ is the indicator function.

$$F_n(x) = \frac{1}{n}\sum_{i=1}^{n} I_{X_i \le x} \tag{2-9}$$

In this study, to calculate the difference between the data distribution and the chosen distribution, the two-sample Kolmogorov-Smirnov test is applied. Equation (2-10) describes the two-sample K-S test, in which D_n is the distance between two sets of data $F_{1,n}$ and $F_{2,n}$ and $\sup_x$ is the supremum of the set of distances.

$$D_n = \sup_x \left| F_{1,n}(x) - F_{2,n}(x) \right| \tag{2-10}$$

The K-S test is performed with the Matlab function kstest2 (2 sample K-S test). Two values are returned by the test function: h and p. The h value reveals whether the null hypothesis that the two sets of data are the same can be accepted with a significance level of 5%. The p-value is the probability, if the test statistic really were distributed as it would be under the null hypothesis.

2.3 Planning renewable energy

Renewable energy planning mainly involves two sections: reliability assessment and economic evaluation.

Reliability assessment takes into account energy adequacy and power quality. In this study, the isolated grid of Coober Pedy is assumed to be small enough that the generations and loads are assumed to be centralized in one spot. Under this assumption, stability and power quality problems are mainly caused by the power fluctuations of the renewables. Compared to the bulk grid, the fluctuations of renewable generation will exert more severe impact in the remote isolated grid like Coober Pedy [3]. A detailed comparison between impacts of renewable to isolated grid and bulk grid is described in [3]. To reduce such impacts, novel power electronics devices [27][28], generation structure [29] and control strategies [30][31] are developed. The fluctuation effects and ways to reduce it will be discussed in Chapter 3. The assessment of energy adequacy is discussed in [4][21][23]. The quantitative criterion is Loss of Load Probability (LOLP) which will be discussed and tested in Chapter 5.

Economic evaluation will consider the sizing of the generation units and corresponding costs of energy. Costs of energy with varied penetration levels of the two different renewable generations (wind and solar) are calculated and shown in Chapter 5.

3. Stochastic Modeling of Renewable Energy

In this chapter the stochastic models of solar radiation and wind speed are introduced. A new bimodal distribution function is made to fit the solar radiation histogram.

3.1 Processing data files

A set of data files [32] recording the local climate is used to generate the stochastic models. The files include records of solar radiation level and wind speed from 1985 to 1988 in every 20 minutes. The original data are in chronological order. To calculate the histograms of the two renewable energy sources all data are rearranged and the data in the same time spot every month are put into the same column. Thus 12 tables with 24 (hours) columns are made. According to Australia climate characteristics, the twelve months' data are divided into four seasons. In conclusion, each section in a season will include approximately

$$3(20\text{min/hour})\times 30(\text{days/month})\times 3(\text{months/season})\times 4(\text{years})=1080 \text{ data.}$$

3.2 Fitting stochastic distributions

The converted data are fitted with the three distributions introduced in Chapter 2: the Weibull distribution, the beta distribution and the exponential distribution. The three distribution functions are tested by the K-S test.

3.2.1 Fitting wind speed histogram

The typical shape of the wind speed histogram is shown in Fig. 3-1. The histograms are normalized according to the values given in the appendix. Two

distribution functions are tested to fit the histogram: the Weibull distribution and the beta distribution. Table 3-1 shows the results of K-S test for each of the distributions. These results accept the Weibull distributions but reject the beta distribution for modeling wind speed.

Table 3-1 K-S Test Results of Wind Speed Distribution Functions

	Spring	Summer	Fall	Winter
Weibull	Accepted	Accepted	Accepted	Accepted
	$p = 0.2271$	$p = 0.2489$	$p = 0.1994$	$p = 0.1535$
Beta	Rejected	Accepted	Rejected	Rejected
	$p = 0.0460$	$p = 0.0652$	$p = 0.0367$	$p = 0.0190$

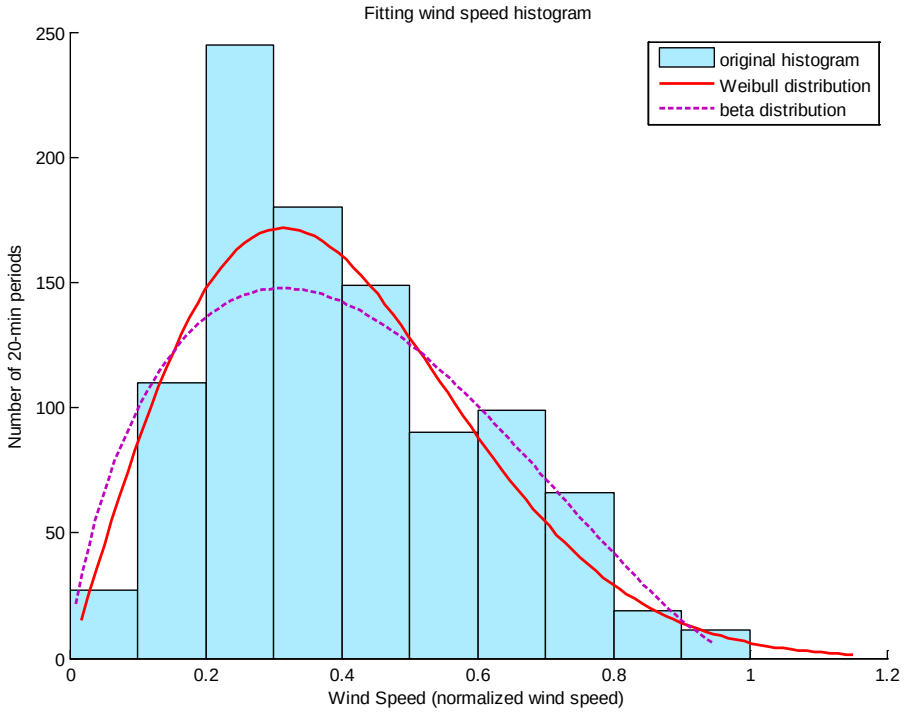

Fig. 3-1 Fitting wind speed histogram.

3.2.2 Fitting solar radiation histogram

Unlike wind speed that has strong correlation during day and night, the solar radiation level may change dramatically in different time spots. The nighttime solar radiation level is always zero or approximately zero.

The histograms of solar radiation level in different hours of different seasons vary considerably. Fig. 3-2 shows the histograms of solar radiation at noon in four seasons. Three distributions are tested: Weibull distribution, beta distribution and exponential distribution. Fig. 3-3 shows fitting of each distribution function.

The K-S test results show that none of the aforementioned distribution functions is acceptable. From Fig. 3-3 it is noticed that the distribution functions are either too large at the minimum or too small at the maximum.

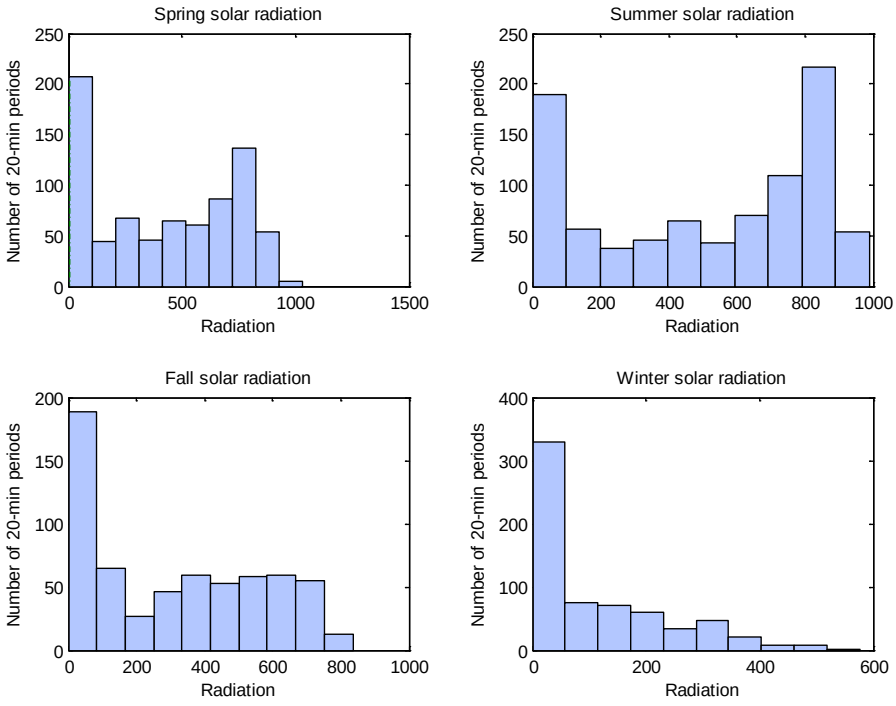

Fig. 3-2 Solar radiation histogram at noon in four seasons.

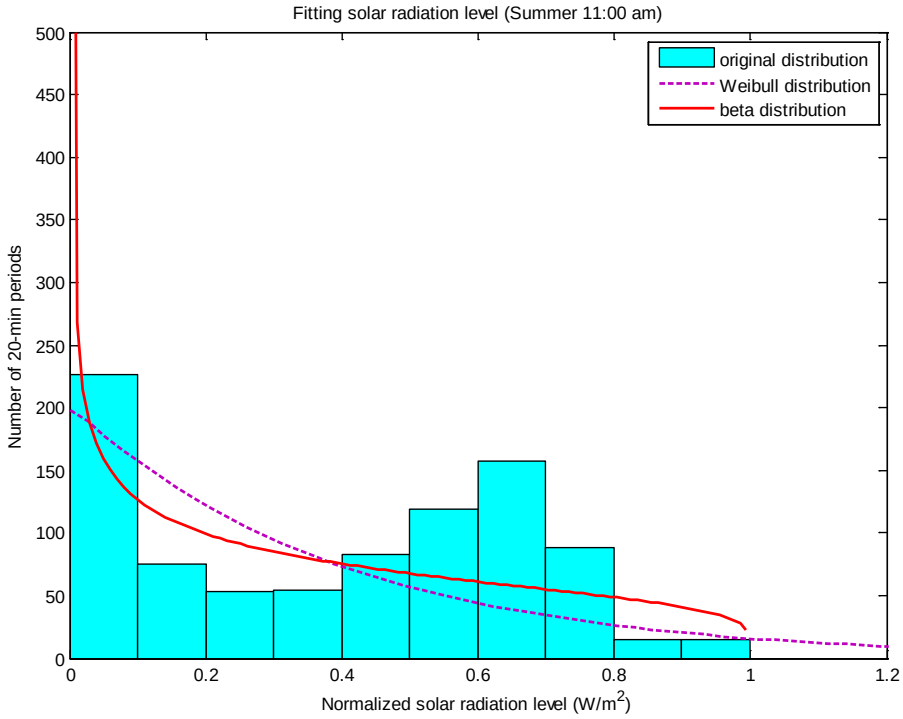

Fig. 3-3 Fitting solar radiation histogram

It can be seen from Fig. 3-3 that the first bar is much higher than the others. It will be more helpful and practical to set up a threshold value and eliminate the data that are lower than this value. In reality solar radiation is measured by the equipment on ground or roof tops, hence, the radiation level should be higher than the diffuse scattered radiation [33] otherwise the sensors may not detect the radiation. The diffuse scattered radiation levels of four seasons in south hemisphere are calculated (shown in next chapter) and set as the threshold value. The new histogram of solar radiation level is shown in Fig. 3-4.

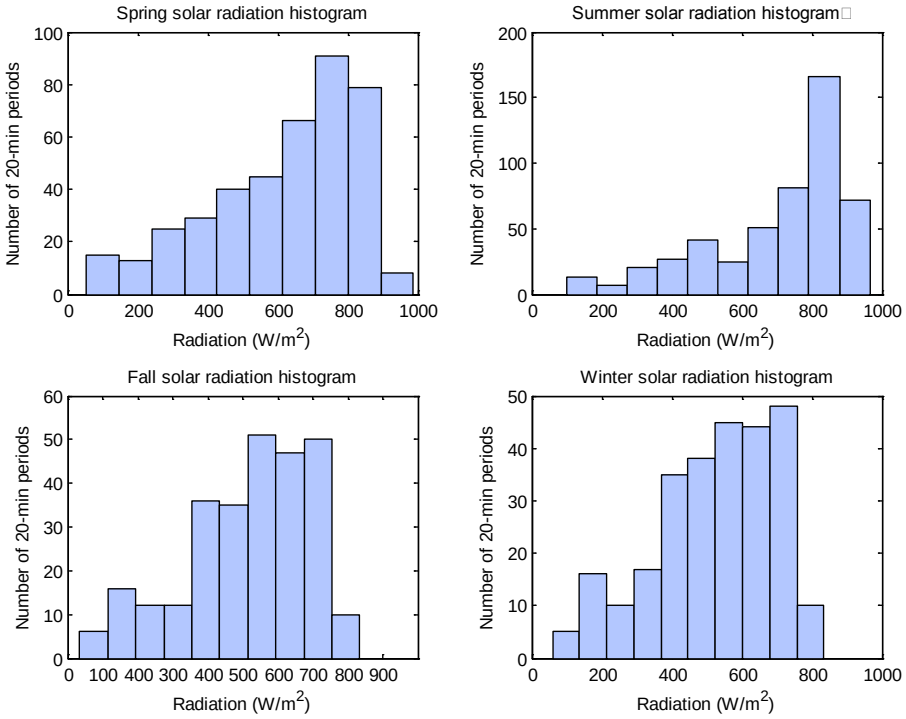

Fig. 3-4 Histogram of modified solar radiation level.

The new histograms are fitted again by the three distribution functions. Test results are shown in Table 3-2, Table 3-3 and Table 3-4. In these tables, if the distributions are accepted over 24 hours, then the distribution is acceptable otherwise the distributions are rejected. The value of p is the average value of the 24 hours test p -value.

Table 3-2 K-S Test Results of Solar Radiation Weibull Distribution

	Spring	Summer	Fall	Winter
Weibull	Rejected	Rejected	Accepted	Accepted
	$p = 0.0041$	$p = 2.3801\times10^{-5}$	$p = 0.0766$	$p = 0.3386$
Beta	Rejected	Rejected	Accepted	Accepted
	$p = 0.0254$	$p = 0.0278$	$p = 0.2059$	$p = 0.1390$

The Weibull distribution and beta distribution can fit the radiation histogram in winter and fall, however neither of them can fit the spring and summer radiation histogram. Fig 3-5 shows the fitness of the distribution for summer solar radiation level at 11:00 am.

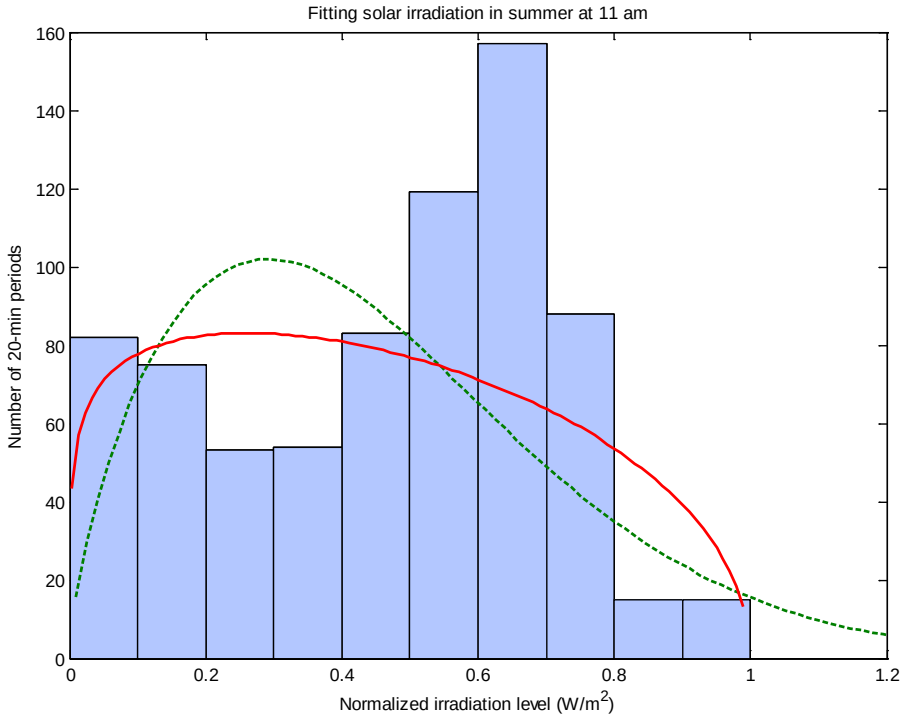

Fig. 3-5 Fitting summer solar radiation level.

3.2.3 A new bimodal distribution

The original distribution, as shown in Fig 3-5, contains two ‘peaks’, namely bimodal, which cannot be fitted by the traditional distribution functions. A new bimodal distribution is introduced to solve the problem.

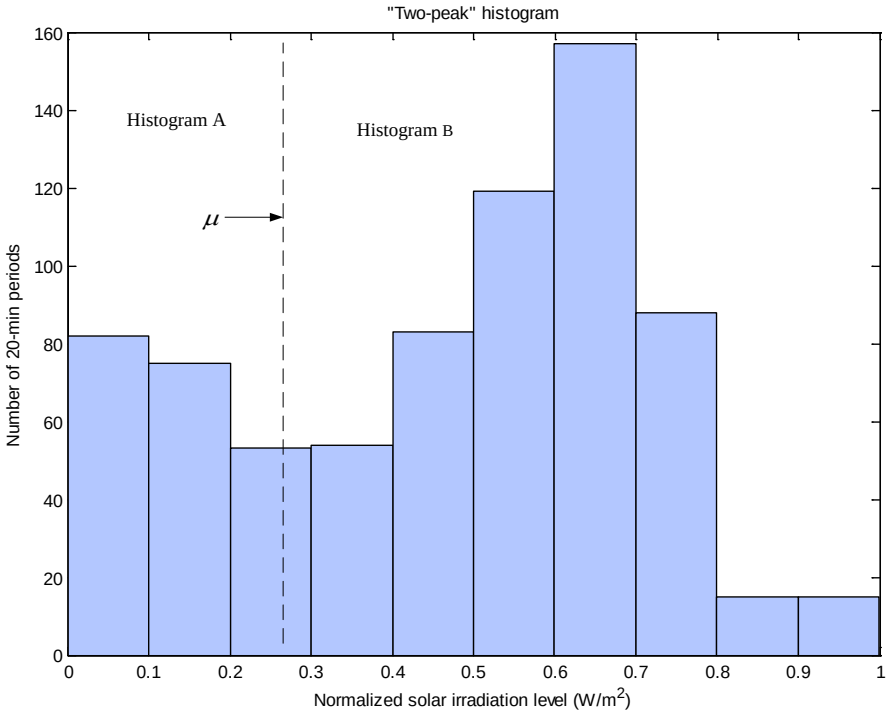

Fig. 3- 6 Divide “two-peak” distribution

As shown in Fig. 3-6 the “two-peak” histogram can be divided into two parts: Histogram A and Histogram B. Two Weibull distributions will fit these two histograms respectively, namely Distribution A and Distribution B. The value of the variable μ, which equals to the column (bin) with minimum distribution frequency, sets up the boundary of the two distributions. The fraction *k* is the portion of the total data that are smaller than μ. With these variables the equation of the bimodal distribution is shown:

$$f(x)=\begin{cases}\dfrac{b_1}{a_1}\left(\dfrac{x}{a_1}\right)^{b_1-1}e^{-(x/a_1)^{b_1}} & 0<r\le k\\ \dfrac{b_2}{a_2}\left(\dfrac{x}{a_2}\right)^{b_2-1}e^{-(x/a_2)^{b_2}} & k<r<1\end{cases}$$

$$r\sim U(0,1) \qquad (3\text{-}1)$$

where r is variable which is randomly given by a uniform distribution $U(0,1)$; a_1, a_2 are shape factors for Distribution A and Distribution B respectively and b_1, b_2 are scaling factors for the two functions, respectively.

The histogram of solar radiation level at 11 am in summer (shown in Fig. 3-5 and Fig. 3-6) is used as an example. For this distribution, μ equals 0.25 and k equals to 0.21. Distribution A and B are respectively shown in Fig. 3-7 and Fig. 3-8.

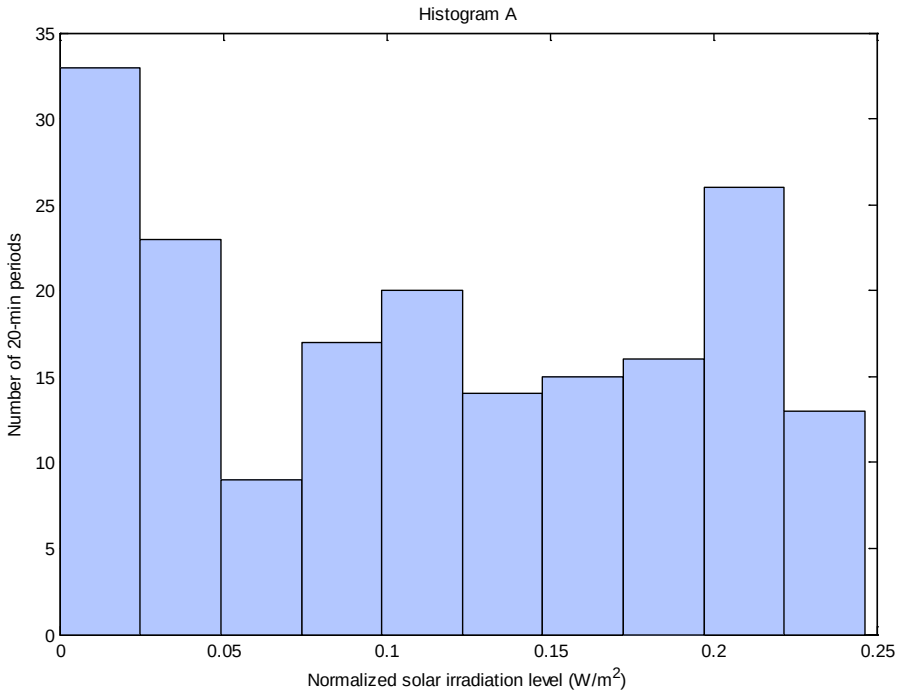

Fig. 3-7 Solar radiation histogram for distribution A.

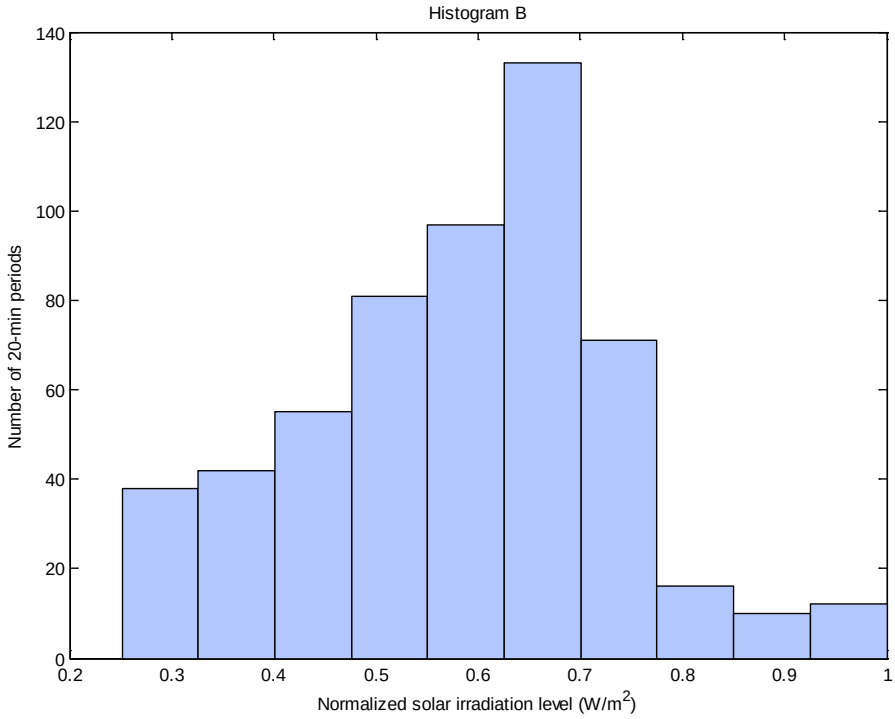

Fig. 3-8 Solar radiation histogram for distribution B.

Shape factors and scaling factors of the two distributions are decided respectively for the two functions, shown in Table 3-3.

Table 3-3 Parameters for Distribution A and Distribution B

	Scaling Factor	Shape Factor
Distribution A	0.1118	1.1600
Distribution B	0.7129	3.9289

The bimodal distribution is accepted by K-S test and the p value is 0.5020 which is much higher than the beta or Weibull distributions. The fitting of the original data distribution with four distribution functions is shown in Fig. 3-9.

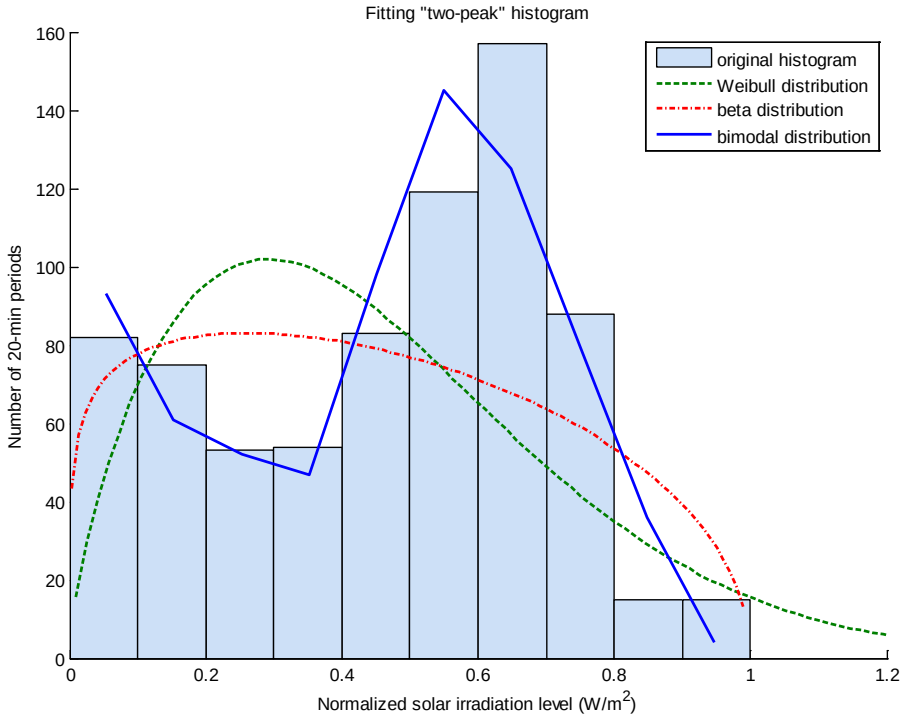

Fig. 3-9 Fitting “two-peak histogram”.

3.3 Conclusion

The stochastic models for wind speed and solar radiation are made in this chapter based on the historical record. With the K-S test choices of distribution functions are made for different sections in different seasons, given in Tables 3-1 and 3-3. A new bimodal distribution which combines two Weibull distributions is used to fit the solar radiation distribution in section 2 of summer. Test results shows that the distribution can fit the original distribution well.

Fig. 3-9 and Fig. 3-10 are minute-by-minute wind generations and PV generations, respectively. These graphs show the renewable generations contain

lots of fluctuations. The effects and methods to deal with such fluctuations will be discussed in Chapter 4.

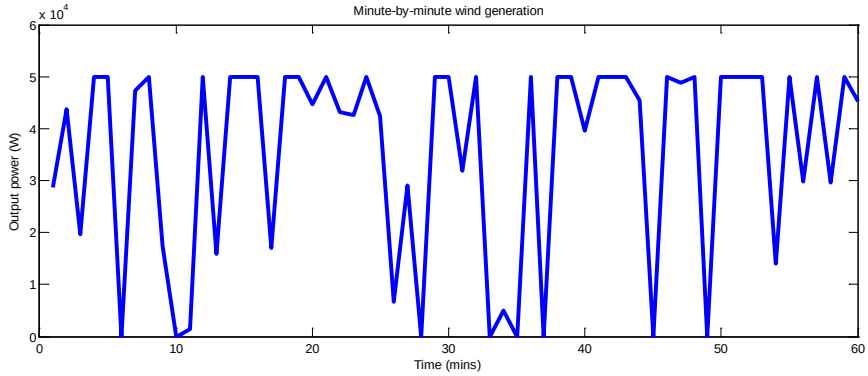

Fig. 3-10 Wind generations.

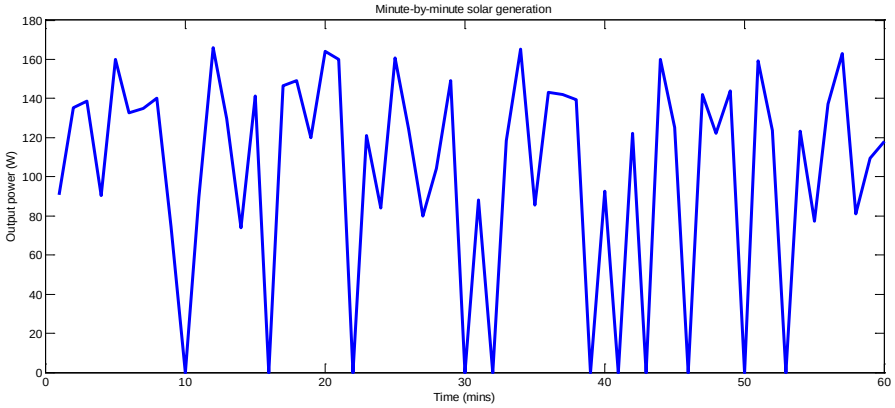

Fig. 3-11 PV generations.

4. Problems with Generation Fluctuations

The models built in Chapter 3 provide hourly wind speed and solar radiation levels which is sufficient for planning. However in practical operations, renewable sources, like solar and wind, are intermittent and the generation may contain high frequency fluctuations, like the minute-by-minute fluctuations shown in Fig. 4-1 and Fig. 4-2. In these graphs, the generation curves are created with the hourly distribution parameters introduced in Chapter 3. A set of hourly parameters is used to create the 60 minutes of generation. Such generation fluctuations may cause frequency deviations, mismatch between generation and demand, and malfunction of devices [34][35][36].

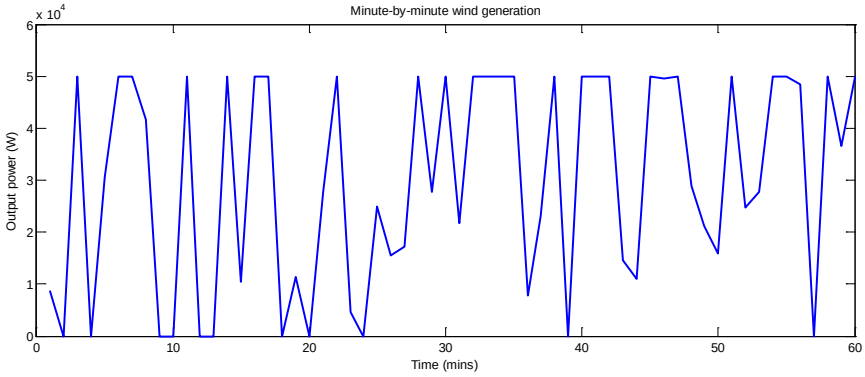

Fig. 4-1 Wind generation fluctuations at noon.

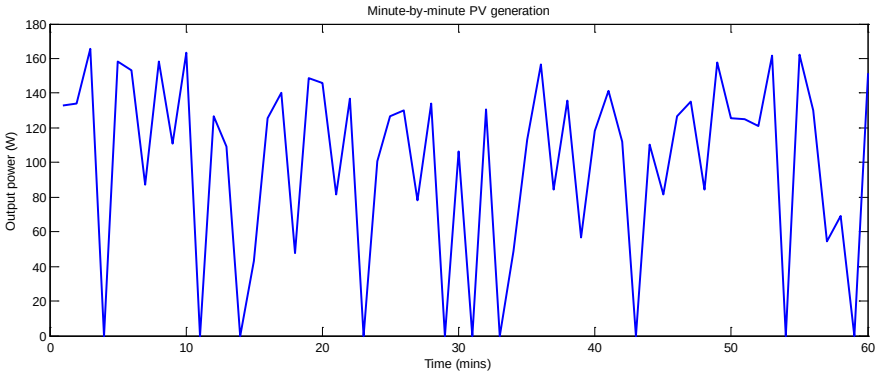

Fig. 4-2 PV generation fluctuations at noon.

In Coober Pedy, the diesel generators (4000 kW) can make sufficient backup power to support the load. However, frequent changes in renewable generation may require frequent start up and shut down of the diesel generators. These switching operations, besides problems with response time, may shorten the lifetime of diesel generators or raise the operation and maintenance (O&M) costs.

In a bulk grid, although larger penetration level may cause stronger fluctuations and bring more significant impact to the system, large scale and wide spread allocation of renewable generation may also reduce the fluctuations since generation varies among the geographically dispersed devices [36]. In Coober Pedy due to the relative small capacity and small area of the plant, all renewable devices are assumed to have identical generation power. The fluctuation should be reduced by other operation methods or devices.

Three main solutions are brought out by the researchers: 1, storage units with appropriate sizing [35]; 2, power limiters [34][37]; and 3, adaptive hierarchical control method [36].

The third method balances the generation based on central and local control commands which adaptively tune the Maximum Power Point of Tracking (MPPT) of the renewable generators. This method is especially useful for the large, complex and mixed-sources system, however it is not applicable in the remote small grid. The following two sections will introduce storage units and limiters.

4.1 Storage unit

Storage units are now commonly used in conjunction with renewable generation [35][36][38][39]. By storing and releasing energy, the storage units can perfectly smooth the renewable generation fluctuations. Moreover, fast storage units like batteries can generate the backup power almost instantly to minimize the generation shortage intervals. The disadvantage of a storage unit is also obvious, high cost is the most significant factor that limits the usage and size of storage. According to data from National Renewable Energy Laboratory (NREL) [40][41], the per kWh costs of a storage unit, using battery as an example, is about $290/kWh. In [42], the cost of storage with CAES (Compressed Air Energy Storage) is calculated as 14 cents/kWh. This cost will raise the local energy costs (44 cents) by 32%. Coober Pedy cannot accept this price especially since there are enough diesel backups. Size evaluation of the storage units in Coober Pedy is still instructive which will give useful information in future planning.

The appropriate sizing of the storage unit tries to balance the generation. Shown in Fig. 4-3, the horizontal straight line indicates the maximum output

power of the generation unit that can be smoothed by a storage unit. The shaded area above the straight line is defined as positive area (storage) and the area under the straight line is defined as negative area (release). The required energy size of storage unit will be the biggest shaded area.

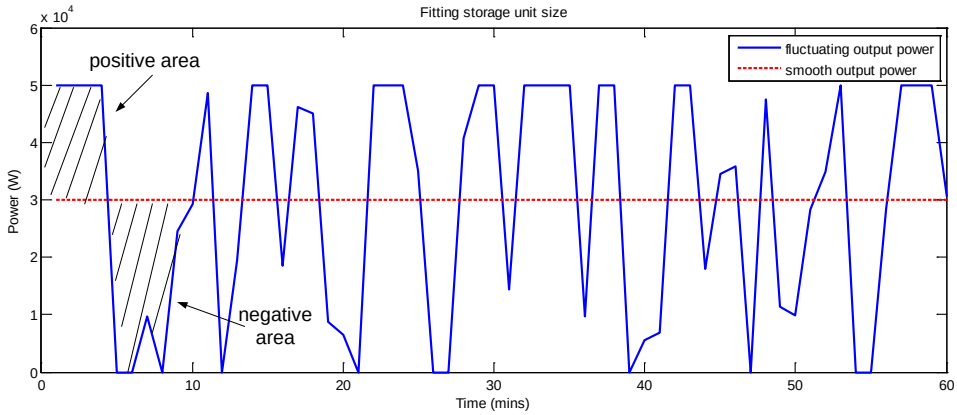

Fig. 4-3 Balancing generation fluctuation.

A full year minute-by-minute simulation is performed to find the appropriate size of the storage unit. Cases with wind and PV generation are studied separately. For PV generation, since it is assumed that PV generation will be zero in the interval from 6 pm to 6 am (the next day), only the PV generation from 6 am to 6 pm is considered in the sizing simulation.

For a 50 kW wind turbine, the maximum smooth generation power is 27.7 kW and for a unit area PV panel (275 W rating power), the maximum smooth generation power is 50 W. The scenario with the 1000 kW renewable penetration is studied based on the aforementioned, and the results are shown in Table 4-1.

Table 4-1 Smooth Generation Power and Storage Sizes (1000 kW penetration)

	Smooth generation power (kW)	Required storage sizes (kWh)
Wind	554	4595.0
PV	175	3717.9

Based on the per kWh costs, in the 1000 kW penetration case, storage costs for wind generation is $\$1.560\times10^6$ (in this thesis, the sign $ stands for US dollars) and for PV generation, the cost is $\$1.345\times10^6$. These two costs are prohibitive for Coober Pedy.

4.2 Power limiter

In references [34][37], several types of power limiters are introduced to reduce fluctuation. In this study, the absolute power limiter is considered. When generated power is higher than the threshold value, power limiters curtail the excessive power and when the generated power is less than the threshold value, diesel generators switch on to replenish the power. Besides reducing generation fluctuation, it is also a goal to maintain a relative high capacity factor.

From Fig. 4-1 and Fig. 4-2 it is seen that the fluctuations are too frequent and dramatic. Using an absolute limiter to smooth power generation may have to curtail all the generation which is unacceptable.

4.3 Discussions

The generations shown in Fig. 4-1 to Fig. 4-3 contain a great deal of fluctuations. The generation values are independently and randomly given by stochastic models in every minute. However, in reality, the wind speed or solar generation in different minutes are correlated, which means the generation will not change dramatically unless extreme weather cases like a wind gust occur. If a complex grid structure and model are built, the absolute power limiter still has the potential to be used in a large grid.

There are eight diesel generator sets in Coober Pedy each has 500 kW capacity. In practical use, a Unit Commitment (UC) schedule can be developed to keep the diesel generator running appropriately and reduce the fluctuation. Due to the lack of practical operation data, a detailed UC scheme is beyond the scope of the study.

The following chapter will model the renewable generation and analyze it for economic planning. Fluctuations are assumed to be reduced by the diesel generators. Storage units and limiters are not considered in the simulations since they are too expensive or impractical. Besides, to limit the impact due to the fluctuation the maximum renewable penetration level is nominally set to be 1050 kW.

5. Planning Renewable Energy

In this chapter the generation and load models are built. The economical planning is done with Monte Carlo simulation.

5.1 Generation and load modeling

5.1.1 Wind generation modeling

The wind turbine output power equation is introduced in Equation (2-2). In this study two types of wind turbine generators (WTG) are considered: a 50 kW wind turbine and a 1.5 MW wind turbine. Data for these two turbines are shown in Table 5-1.

Table 5-1 Data of Wind Turbines

Parameters	50 kW WTG	1.5 MW WTG
Cut in speed (m/sec)	2	5
Cut out speed (m/sec)	20	15
Rated speed (m/sec)	9	10

5.1.2 PV generation modeling

The basic equation of PV output power is given in Equation (2-3). In the study, the output of a unit area solar panel is calculated (A=1); η_p is assumed to be 15% [28].

The calculation of R is:

$$
\begin{aligned}
R &= I_D + I_{DS} + I_{DR} \\
I_D &= I_{DN}\cos(\theta) \\
I_{DS} &= CI_{DN}\left[\frac{1+\cos(\beta_2)}{2}\right] \\
I_{DR} &= I_{DN}\rho(C+\sin(\beta_1))\left[\frac{1-\cos(\beta_2)}{2}\right]
\end{aligned}
\tag{5-1}
$$

where I_D , I_{DS} and I_{DR} respectively represent the direct radiation flux, diffuse scattered radiation and reflected radiation, respectively. Reflected radiation is always much smaller than the other two components and is neglected in the calculation. C is the ratio of diffuse radiation on a horizontal surface to the direct normal irradiation. β_1 is the altitude angle and β_2 is the collector tilt angle. The collector angle, θ , is calculated by:

$$\cos\theta = \sin(\beta_1)\cos(\beta_2) + \cos(\beta_1)\sin(\beta_2)\cos(\alpha_1 - \alpha_2) \tag{5-2}$$

where α_1 is the azimuth angle and α_2 is the collector rotational angle.

Due to the elliptical Earth orbit of revolution, the solar angles (α_1 and β_1) vary with time and position. The solar time can be described by the solar hour angle H :

$$H = \frac{AST - 720}{4} \tag{5-3}$$

where AST is the apparent solar time [43].

The altitude angle can be calculated using:

$$\sin(\beta_1) = \cos(L)\cos(\delta)\cos(H) + \sin(L)\sin(\delta) \tag{5-4}$$

where L is the local latitude (negative in southern hemisphere); δ is the declination.

The azimuth angle can be calculated:

$$\cos(\alpha_1) = sign(L)\frac{\sin(\delta)-\sin(\beta_1)\sin(L)}{\cos(\beta_1)\cos(L)} \tag{5-5}$$

In Equation 5-5, the factor $sign(L)$ equals to -1 in case of southern hemisphere. The collector angles depend on the type of panel. For dual-axis tracking panels, α_2 and β_2 are equal to α_1 and β_1 respectively. For single-axis tracking panels one of the collector angles will track the solar angle but the other one will remain fixed. For fixed panels both of the two collector angles are fixed.

In (5-1) I_{DN} is the direct normal radiation:

$$I_{DN} = I_0 \exp\left(-\frac{\rho}{\rho_0}\frac{B}{\sin(\beta_1)}\right) \tag{5-6}$$

where I_0 is the apparent radiation which is a function of the day of the year (I_0 on the typical day of each season is shown in Table 5-2); $\frac{\rho}{\rho_0}$ is the pressure at the location of interest relative to the standard atmosphere, and depends on the local elevation; and B is the atmospheric extinction coefficient.

Table 5-2 Value of Solar Variables in Each Season*

Season (Date)	I_0 (W/m^2)	δ (degree)	B	C
Spring (Oct 15)	1173.7	-9.23	0.1800	0.0970
Summer (Jan 15)	1154.1	-21.27	0.2070	0.1360
Fall (April 15)	1154.0	9.41	0.1600	0.0730
Winter (July 15)	1156.9	21.52	0.1420	0.0580

*Value of the variables are converted to southern hemisphere

The value of irradiation in each season for the three kinds of panels can be determined. For the single-axis panels, two types of panels are tested with tilt angle (β_2) and rotational angle (α_2) ranging from zero to ninety degrees. The summation of a whole day's outputs is calculated with different fixed angles, shown in Fig. 5-1 and Fig. 5-2.

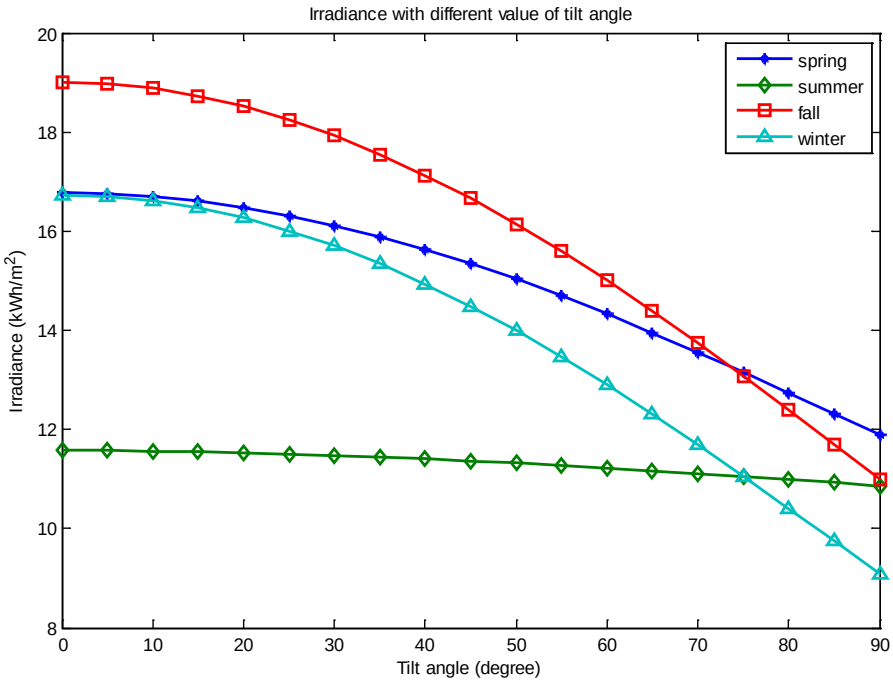

Fig. 5-1 Irradiation on collector surface with different tilt angles.

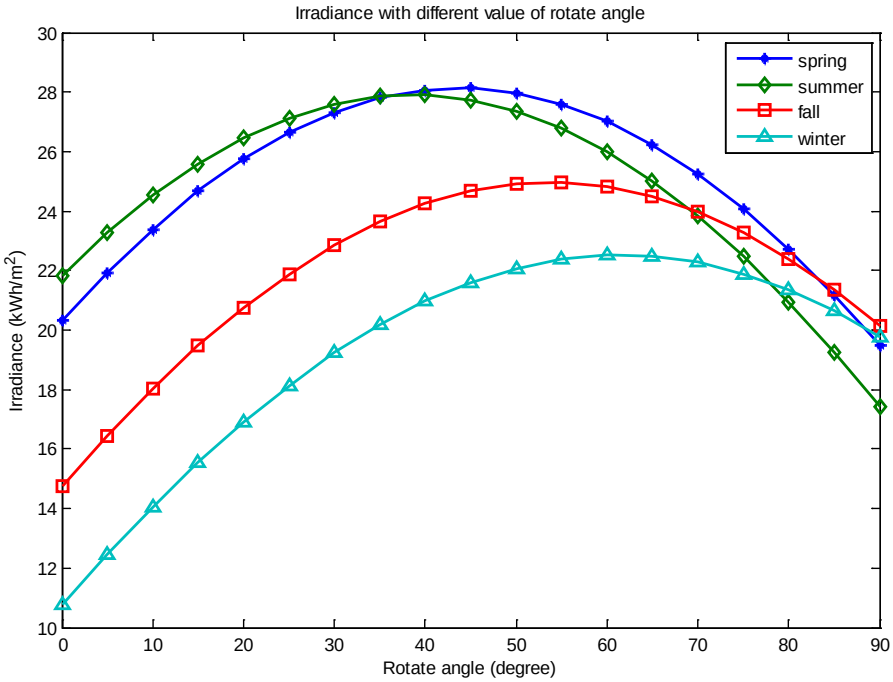

Fig. 5-2 Irradiation on collector surface with different rotational angles.

In the further planning analysis, the single-axis model is used. As observed from Fig. 5-1 and Fig. 5-2, the panels which can track tilt angle and have fixed rotational angle equal to 45° will have the best output. Using the dual-axis output as the benchmark, ratios quantifying the energy outputs for single-axis and fixed panels are created.

$$k_{PV} = \frac{\sum_{i=1}^{24} P_{PV-1i}}{\sum_{h=1}^{24} P_{PV-2h}} \tag{5-7}$$

where P_{PV-1} and P_{PV-2} are the single-axis output and dual-axis panel output respectively; k_{PV} is the ratio; i and h are hours.

Fig. 5-3 and Fig. 5-4 show the hourly radiation level on the dual-axis panel and the single axis panel, respectively. The calculated value shows the ratio for the rotational angle fixed (rotational angle equals to 45º) panels is 95% and for the tilt angle fixed (tilt angle equals to 0º) panels is 50%. The former type is preferred and used in the study because of its higher efficiency.

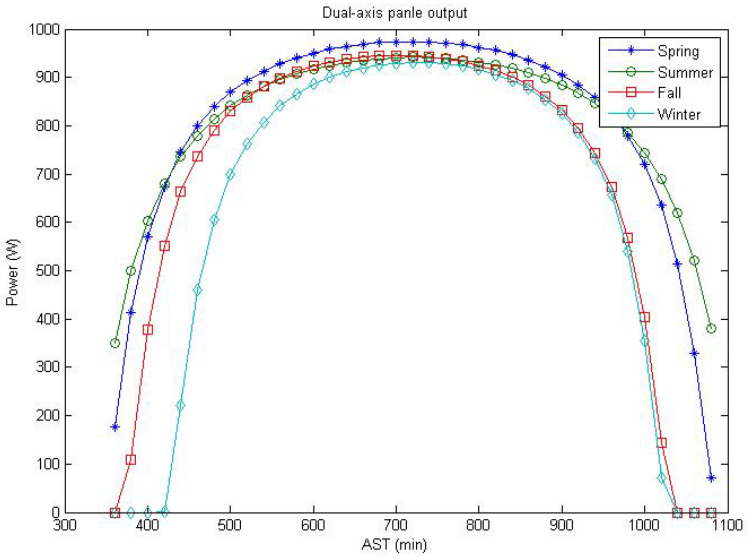

Fig. 5-3 Hourly radiation level on dual-axis panels.

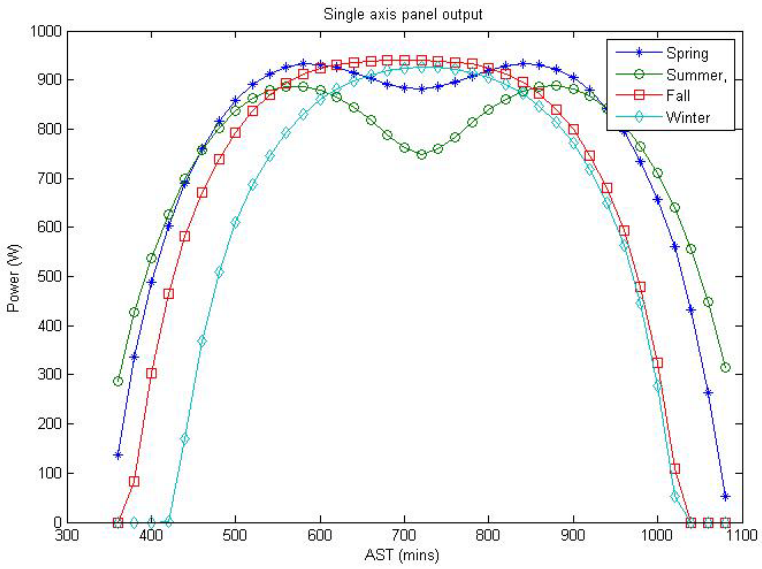

Fig. 5-4 Radiation level on single-axis panels.

In subsequent calculations, the output of a PV panel can be determined by:

$$P_{PV} = rk_{PV} \tag{5-8}$$

where r is the radiation level given by the stochastic model.

5.1.3 Load modeling

Unlike wind and PV generation modeling, the load is not modeled by distribution functions. The original load data are a weekly data set, shown in Fig. 5-5. For each season, there are 7 data for an hour which is not enough to create a meaningful histogram of the data distribution function. Hence in the simulations, the hourly load value is randomly picked from the corresponding 7 values. From Fig. 5-5 it is also shown that the summer load in Coober Pedy is much higher than the other seasons which will bring more concerns on the reliability issues.

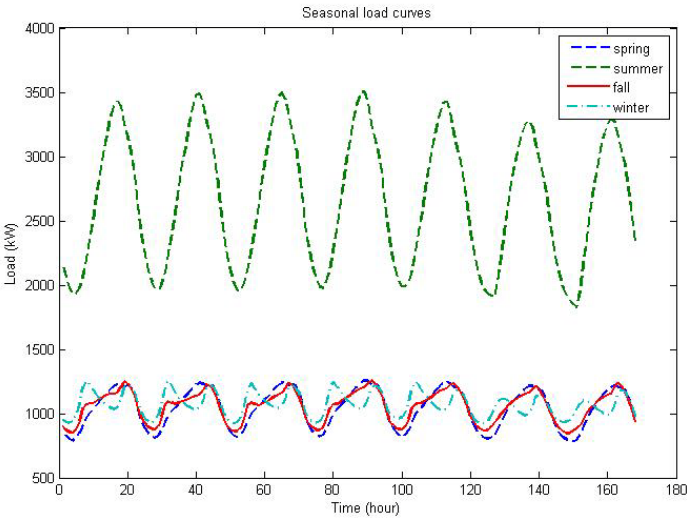

Fig. 5-5 Seasonal load curves.

5.2 Monte Carlo simulation

5.2.1 Introduction

Monte Carlo simulation (MCS) is a simulation method that relies on repeated random sampling to compute the results. In this study due to the intermittent generation of renewables, hourly simulation is performed to test the system reliability and also calculate the costs with different penetration levels.

Due to the variation of the load and renewable sources, hourly simulation is done. For a one-year simulation, there will be 8760 steps and in every step, random values of the renewable generation and load will be given by the stochastic models.

Two results are given in the study: system reliability and costs per kWh energy. In Cooper Pedy, there are originally eight 500 kW diesel generation sets

and the peak load (in summer) is about 3.5 MW, in other words, there is sufficient diesel generation sets to backup the load.

Two scenarios are set in the test: 1, comparing the load and generation level hourly without excluding any diesel set; 2, comparing the load and generation level while excluding a certain amount of diesel sets. The test results are shown in next section. For economic analysis, total costs including capital costs, operation and maintenance (O&M) costs, and fuel costs are calculated with different penetration levels.

5.2.2 Reliability tests

In scenario one, due to the sufficient diesel generation reserve, the LOLP (loss of load probability) of the system will always be zero. Renewable generation is assigned to support a proportion of the total load. Based on the local government's report, 30% (1050 kW) is the maximum penetration level otherwise stability and power quality will be deteriorated. Instead of LOLP, the capacity factor is calculated in scenario 1 with varied penetration levels and sources.

Table 5-3 shows that wind generation has significantly higher capacity factor than PV generation.

Table 5-3 Capacity Factor with Varied PV and Wind Penetration

Penetration level (kW)	Capacity factor (%)	
	Wind	PV
175	42.3%	10.3%
350	40.3%	10.3%
525	40.3%	10.3%
700	40.3%	10.3%
875	40.3%	10.3%
1050	40.3%	10.4%

In scenario two, a certain amount of diesel generation is excluded from the system. In this case, the costs of per kWh energy can be lowered since some O&M costs are avoided; however, the LOLP of the system will not remain at zero.

The same renewable penetration range is tested in scenario two. The margin between the total load and the total generation (including diesels and renewable) is calculated. The cases include excluding one diesel generator and excluding two diesel generators. Table 5-4 shows the value of LOLP with various penetration levels.

Table 5-4 LOLP of Scenario 2

Penetration level (kW)	PV		Wind	
	Exclude 1	Exclude 2	Exclude 1	Exclude 2
175	0.00016	0.08	0.00016	0.06
350	0.00011	0.07	0.00016	0.05
525	0.00011	0.07	0.00011	0.04
700	0.00010	0.06	0.00009	0.03
875	0.00010	0.06	0.00009	0.02
1050	0.00008	0.05	0.00005	0.02

Shown in Table 5-4, when 2 diesel generators are excluded the lowest LOLP is 0.02 which means 174.2 hours loss of load in a year. This LOLP is unacceptable. In case of excluding one diesel unit, the LOLP for PV and wind penetration can be as low as 0.00008 (0.7 hrs/year) and 0.00005 (0.44 hrs/year) respectively. This LOLP (less than 1 hour a year) is acceptable. The highest LOLP, with 375 kW penetration level, is 0.00016 (1.4 hrs/year). This penetration level is not hard for people to accept.

It is also instructive to show the seasonal generation and load curves with the two renewable sources. In Fig. 5-6 and Fig. 5-7 each season is represented by 24 hours, and the data value is the mean value of all data in the same hour. 96 data are included in each graph, from spring to winter. It is shown that the generation curve shape is similar to the load curve shape in most of the times. However, summer peak load is overly high, which requires high diesel generation backup.

Since the load level in Coober Pedy is relatively small, hence it is not practical to integrate both wind and PV generation. The goal of the study is to find the better generation source between wind and PV.

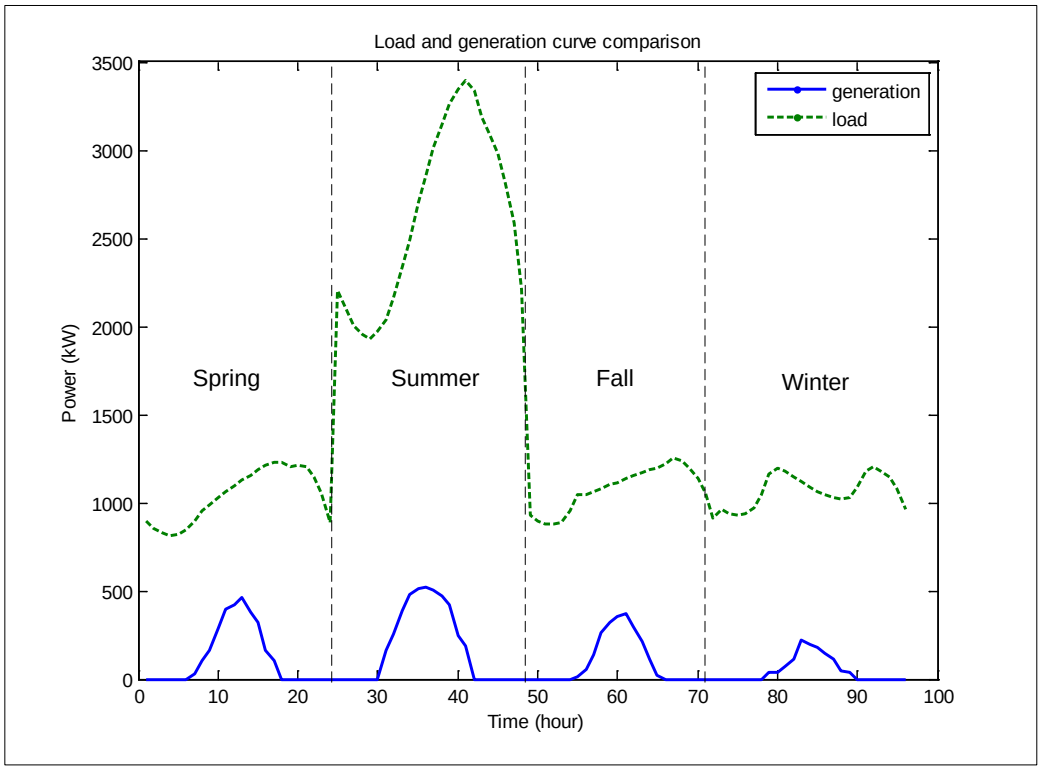

Fig. 5-6 PV output and load curves.

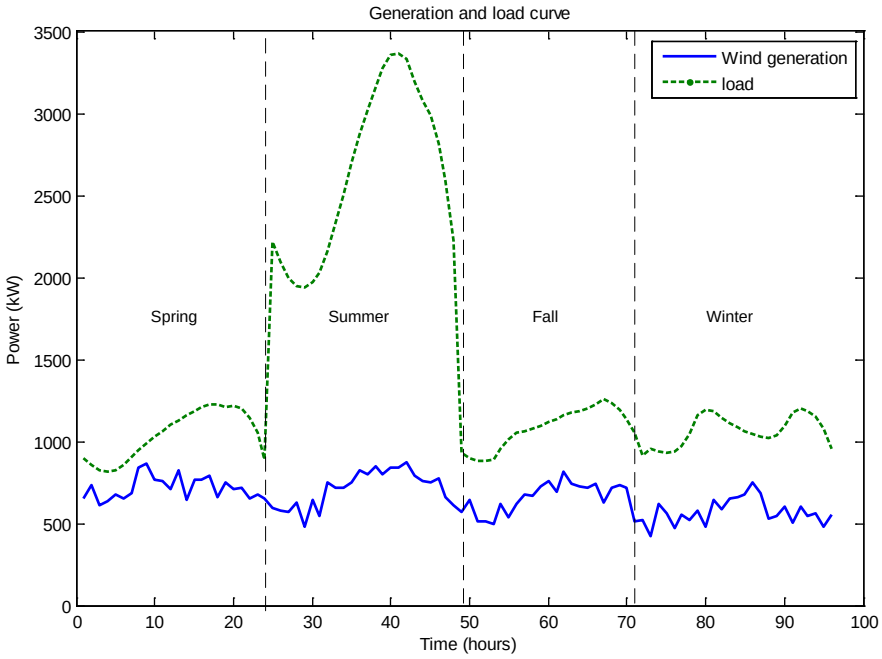

Fig. 5-7 Wind output and load curves.

5.2.3 Economic analysis

In this section the costs issues are studied. The generation costs of the system include capital costs, O&M costs and fuel costs. The data of costs are shown in Table 5-5. The data of capital costs for PV and O&M costs for both PV and wind plants are obtained from a National Renewable Energy Laboratory (NREL) report [5]. Wind generation capital costs are strongly related to the turbine sizes, blade materials, rotor radius, etc [44]. In this study it is assumed that 50 kW turbines are used, and based on data from the Department of Energy (DOE) [45], the capital cost for wind generation is $2500/kW. The capital costs can be converted to per kWh energy costs with:

$$e_C = \frac{IF_B}{P_{e,rate} CF (8760 hrs / yr)} \tag{5-9}$$

where $F_B / P_{e,rate}$ is the capital cost expressed in terms of dollars per installed kW power; I is the levelized annual fixed charge rate which in this study equals 0.06 and CF is the capacity factor.

Table 5-5 Cost Data for The Three Sources.

	Capital costs ($/kWh)	O&M cost ($/kWh)	Fuel cost ($/kWh)	Total Costs ($/kWh)
Diesel	0*	0.04 [1]	0.40 [1]	0.44
PV	0.46 [5]	0.01 [5]	0	0.47
Wind	0.096 [45]	0.02 [5]	0	0.116

*This analysis assumes that the existing diesel generators are already completely paid for.

From Table 5-5, PV costs are higher than the diesel costs and wind is cheaper than diesel costs. It is obvious that the total cost of PV generation is higher than diesel and wind. However it is still instructive to show the results with PV penetration to give a numerical comparison between the three sources. In addition since the O&M cost of PV generation is relatively lower than other two sources, PV generation has the potential to be cheaper than diesel or wind after all capital costs are paid back. This long term cost comparison will be shown in the next section.

Similar to the reliability analysis, two scenarios are studied (without and with diesel generators excluded). Shown in Fig. 5-8 and Fig. 5-9 with no diesel generator excluded, in the case of PV penetration, the price increases from

$0.44/kWh to $0.442/kWh while with wind penetration, the price can be lowered to $0.35/kWhf. In order to illustrate relationship between cost and generation better, the simulations are run ten times. In the following figures (Fig. 5-8 to Fig. 5-13), ten curves are shown in each graph.

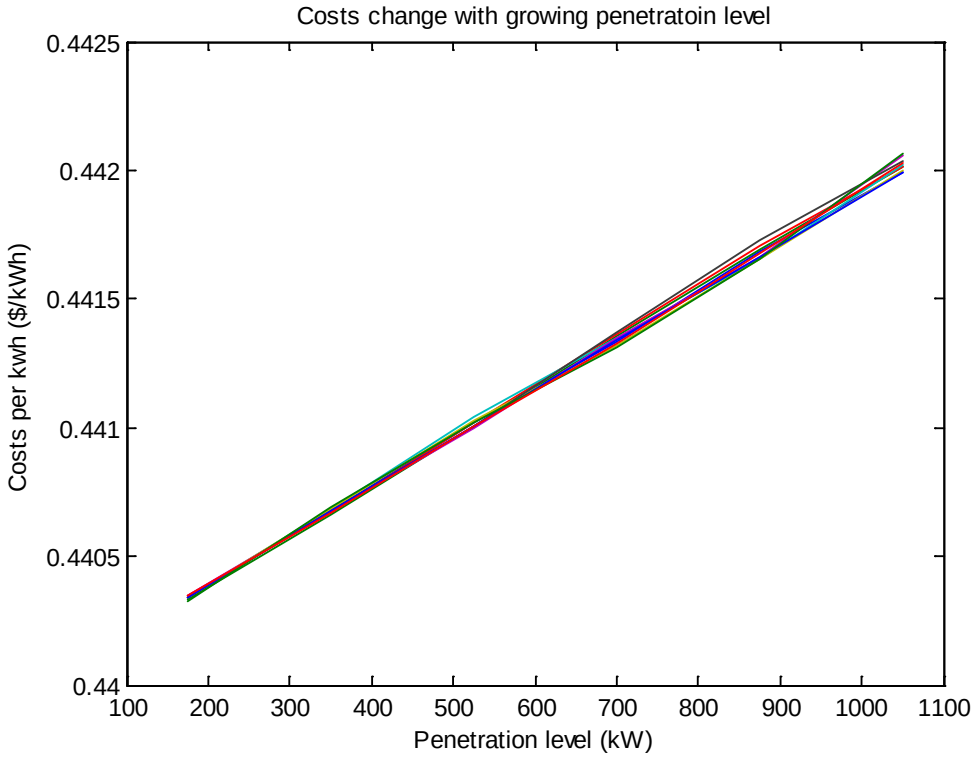

Fig. 5-8 Energy costs with PV penetration in scenario 1.

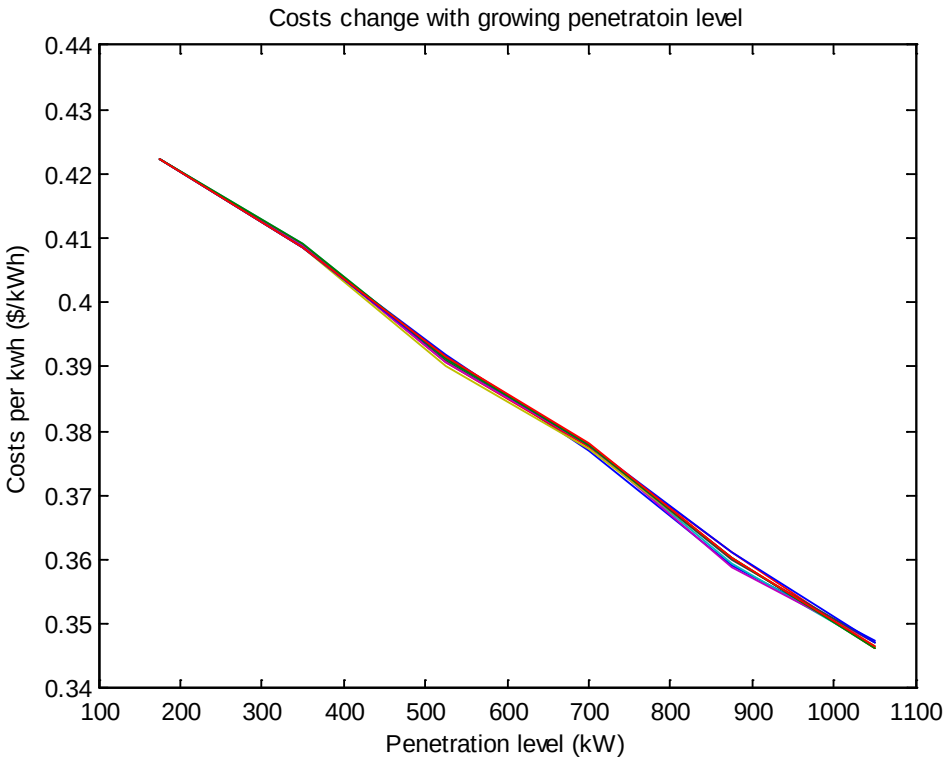

Fig. 5-9 Energy costs with wind penetration in scenario 1.

Scenario two is more economical. In Table 5-5 the diesel O&M cost is given by local government report. Since, without renewable generation, there are eight 500 kW diesel turbines and the average load is 1256 kW in Coober Pedy. It is assumed the local diesel capacity factor is 31%. With this assumption and based on Equation (5-12), the one-year O&M cost for Coober Pedy is calculated and equals to \$105/yr. Costs and capacity factors in cases of excluding one and two diesel generators are calculated and shown in Table 5-6. If, with renewable penetration, a certain amount of diesel generators are excluded, the diesel capacity factor will be increased and per kWh O&M cost will be lowered.

$$e_{O\&M} = \frac{P_{O\&M}(\$/yr)}{CF \times 8760(hrs/yr)} \tag{5-10}$$

Table 5-6 Diesel Generation Capacity Factor and O&M Costs in Exclusion Cases

Number of Diesel Generators Excluded	Capacity Factor	O&M cost ($/kWh)
1	0.36	0.033
2	0.42	0.028

Energy costs with PV and wind penetration in cases with 1 diesel generator or 2 diesel generators excluded are shown from Fig. 5-10 to Fig. 5-13. Tables 5-7 and 5-8 show the energy costs with different penetration levels of the two renewable sources.

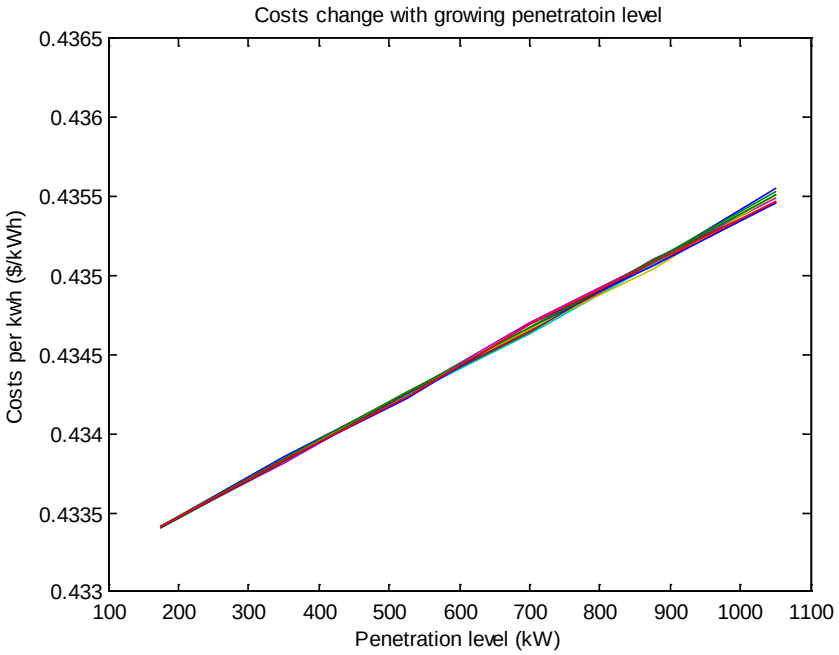

Fig. 5-10 Energy costs with PV penetration (1 diesel generator excluded).

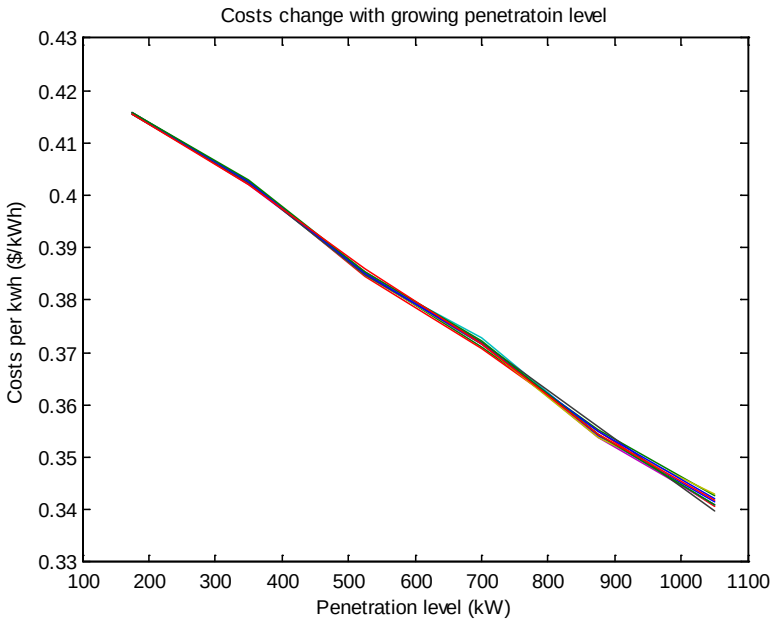

Fig. 5-11 Energy costs with wind penetration (1 diesel generator excluded).

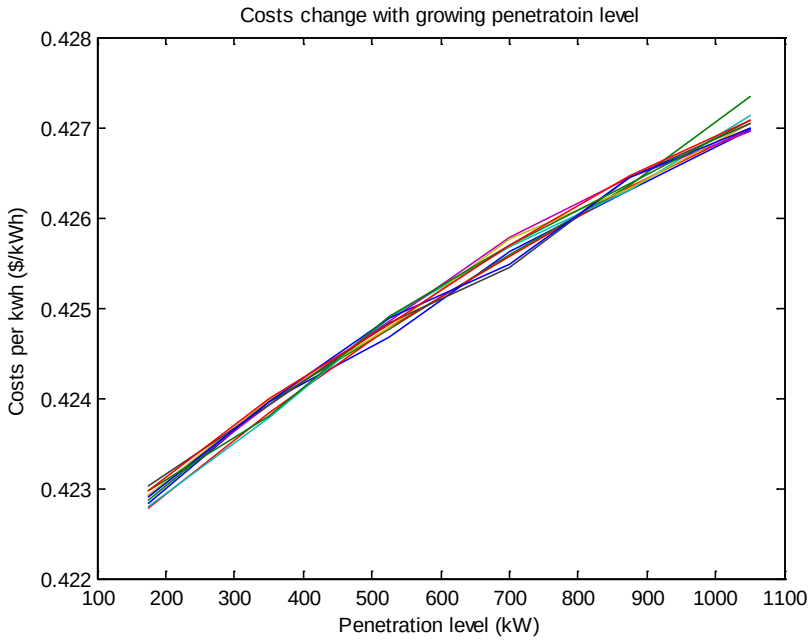

Fig. 5-12 Energy costs with PV penetration (2 diesel generators excluded).

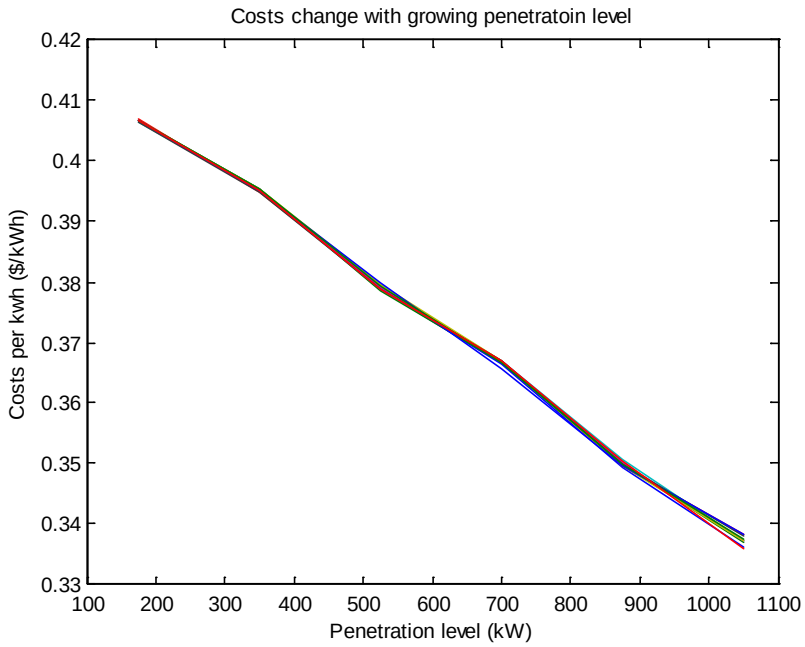

Fig. 5-13 Energy costs with wind penetration (2 diesel generators excluded).

Table 5-7 Average Energy Costs with 1 Diesel Generator Excluded

Renewable Type	Costs ($/kWh) with varied penetration levels (kW)					
	175kW	350kW	525kW	700kW	875kW	1050kW
PV	0.4334	0.4338	0.4342	0.4347	0.4351	0.4355
Wind	0.4154	0.4022	0.3858	0.3716	0.3543	0.3417

Table 5-8 Average Energy Costs with 2 Diesel Generators Excluded

Renewable Type	Costs ($/kWh) with varied penetration levels (kW)					
	175kW	350kW	525kW	700kW	875kW	1050kW
PV	0.4228	0.4236	0.4246	0.4253	0.4260	0.4266
Wind	0.4171	0.3999	0.3746	0.3600	0.3355	0.3185

With no diesel unit excluded the costs with wind penetration reduced from $0.4171/kWh to $0.3417/kWh while with PV penetration the costs increased from $0.4334/kWh to $0.4355/kWh.

5.3 Conclusion and discussion

5.3.1 Long term and short term selection

Shown from the aforementioned results with higher penetration rate, the energy costs with PV penetration are growing while wind generation costs keep reducing. Hence 1050 kW wind penetration will be the most economical solution. The aforementioned results are all based on the assumption that the payback period is 10 years. From Table 5-5 O&M costs of PV generation is lower than wind generation, hence after 10 years when the capital costs are paid back, the cost of PV generation is potentially lower than wind generation, Table 5-9 shows the results after 10 years when capital costs are paid back.

Table 5-9 Energy Costs without Capital Costs

Renewable Type	Costs ($/kWh) with different penetration level (kW)					
	175kW	350kW	525kW	700kW	875kW	1050kW
PV	0.4282	0.4234	0.4190	0.4140	0.4091	0.4046
Wind	0.4102	0.3930	0.3714	0.3531	0.3297	0.3116

Shown in Table 5-9 the PV costs without capital costs are still higher than wind generation costs. This is because of the low capacity factor of PV generation and the requirement of larger amount of diesel generation. In summary, wind

generation no matter in short term or long term is more beneficial than PV generation.

5.3.2 Extreme cases of PV penetration

The climate in Coober Pedy is always dry and hot. Based on a 30 years database of local climate, there are about 28.6 rainy days in a year (365 days). Hence there is about 7% possibility that the PV generation may not be available. Table 5-10 shows the results with 1 diesel unit dropped while considering the factor of extreme weather cases.

Table 5-10 Costs and Payback with PV Penetration (1 diesel unit dropped)

	Penetration level (kW)					
	175	350	525	700	875	1050
Costs ($/kWh)	0.4334	0.4338	0.4342	0.4348	0.4351	0.4356
LOLP	0.00016	0.00013	0.00011	0.00011	0.00011	0.00011

Compared to the results shown in Table 5-7 and Table 5-10 the cost is reduced and the LOLP is higher (original LOLP is 0.00008). The change scale is small and can be neglected.

5.3.3 Appropriate level of penetration

The local government states that 250 kW wind penetration is the best. Compared to the suggestion made in this study, the government's suggestion is more conservative. This may be because of the concerns of power fluctuation discussed in Chapter 4. Fig. 5-7 shows the generation and load curves with 1050

kW penetration, the renewable generation may take more than 30% load. In Fig. 5-14, the curves of wind generation and load are shown with penetration of 350 kW. The average load level is 1256 kW [1], 350 kW is closer to 30% which may make the price lower than the costs with 250 kW penetration.

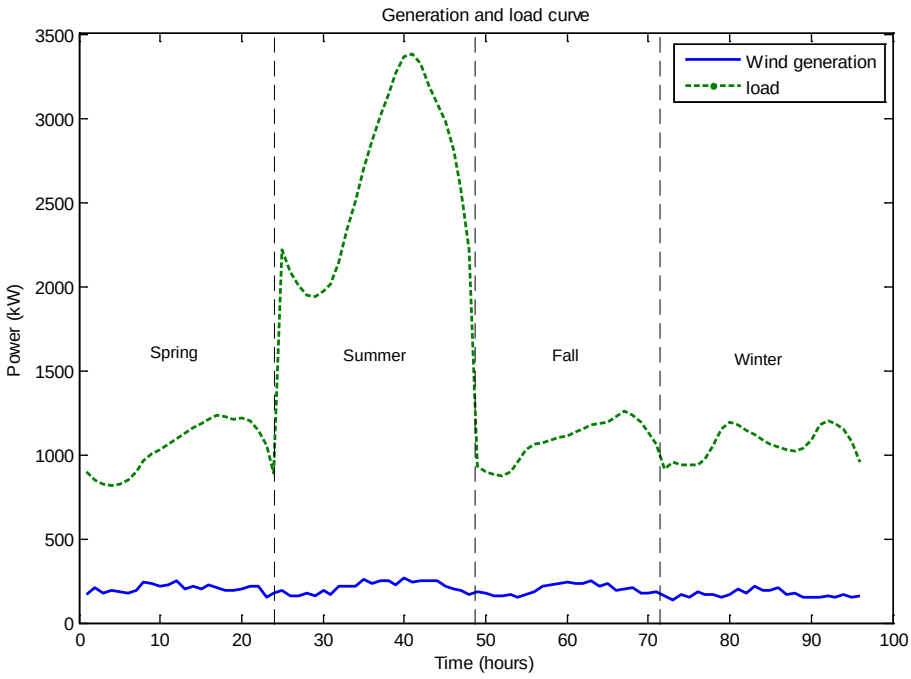

Fig. 5-14 Load and generation curve with 350 kW wind penetration.

In the aforementioned analysis 50 kW wind turbines are selected. It is believed that with larger turbine size, the cost of per kW installed power is lowered. Hence it is worth to consider the case of using a utility scale wind turbine (1.5 MW) to implement the generation. The per kW installed power O&M cost is assumed to be the same as the 50 kW turbine. The capital cost is $1500/kW [46] or $0.055/kWh. A penetration level of 1500 kW is considered and the results are shown in Table 5-11.

Table 5-11 Results in Case of Using 1.5 MW Wind Turbine

Turbine type	1.5 MW	50 kW
Cut in speed (m/s)	2	5
Cut out speed (m/s)	20	15
Efficiency*	97%	92%
Cost ($/kWh)	0.31454	0.30488
Capacity factor	33%	40%
LOLP	0.0004	0.0001

*The efficiency is based on the Betz Efficiency

Compared to the results in Table 5-11 with 1500 kW penetration, the cost is not reduced but increased. This may because the large wind turbine requires larger wind speed which raises the LOLP and lowers the capacity factor. Lower capacity factor will increase the total costs. Hence 50 kW wind turbines are more economical and reliable.

5.3.4 Extra large penetration option

In the aforementioned analysis, the maximum penetration level is set to 1050 kW (30% of the summer peak load). It is shown that the wind costs increase monotonically and the PV energy costs increase monotonically. It is because the high costs of PV generation and low costs of wind generation. What if the penetration level goes larger?

From Fig. 5-15 it is seen when the wind penetration level goes higher (2500 kW), the renewable generation may be greater than the load level. The excessive power is assumed to be curtailed. In this case, capacity factor is lowered. Equation

(5-9) shows that lower capacity factor leads to higher energy costs. Hence, when the penetration level is raised to an extra large level (>1050 kW) the costs may go higher. Observing from Fig. 5-7 and Fig. 5-15, the optimum penetration level will be the level that makes the generation and load best matched. Fig. 5-16 shows the case with PV penetration. It is found that since the capacity factor of PV generation is very low (10%), renewable generation in most times is lower than load. Unlike wind generation, the capacity factor of PV generation will not change significantly until the penetration level reaches very high level (>2800 kW).

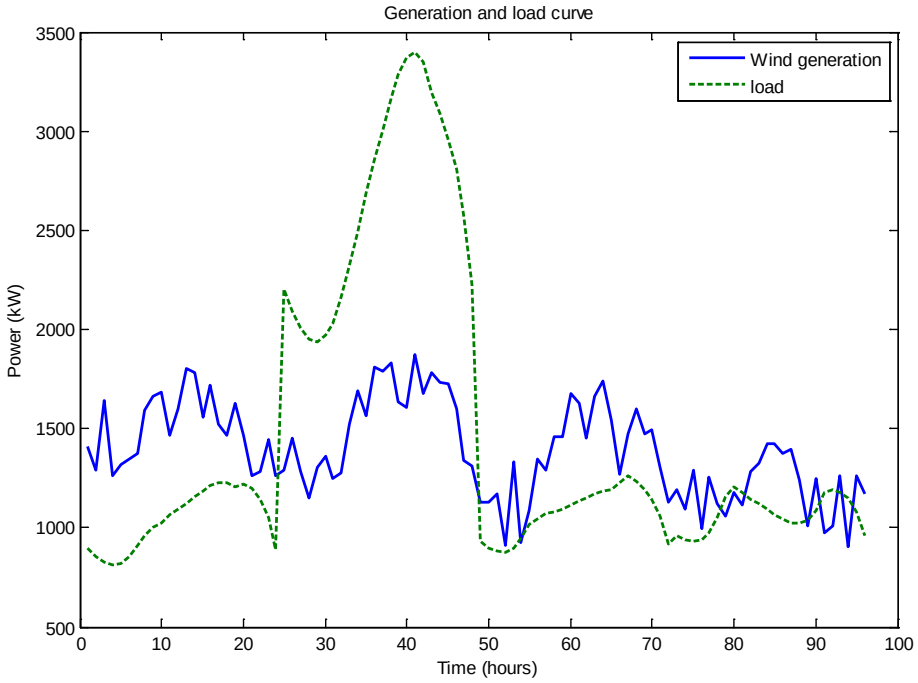

Fig. 5-15 Generation and load curves with 2500 kW wind penetration.

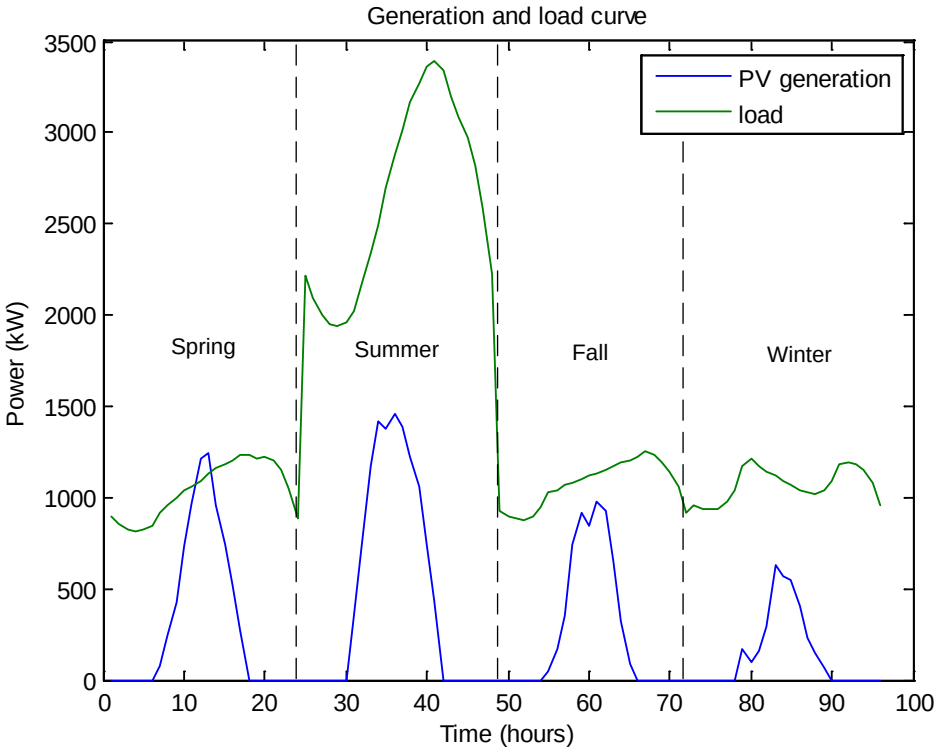

Fig. 5-16 Generation and load curve with 3150 kW PV penetration.

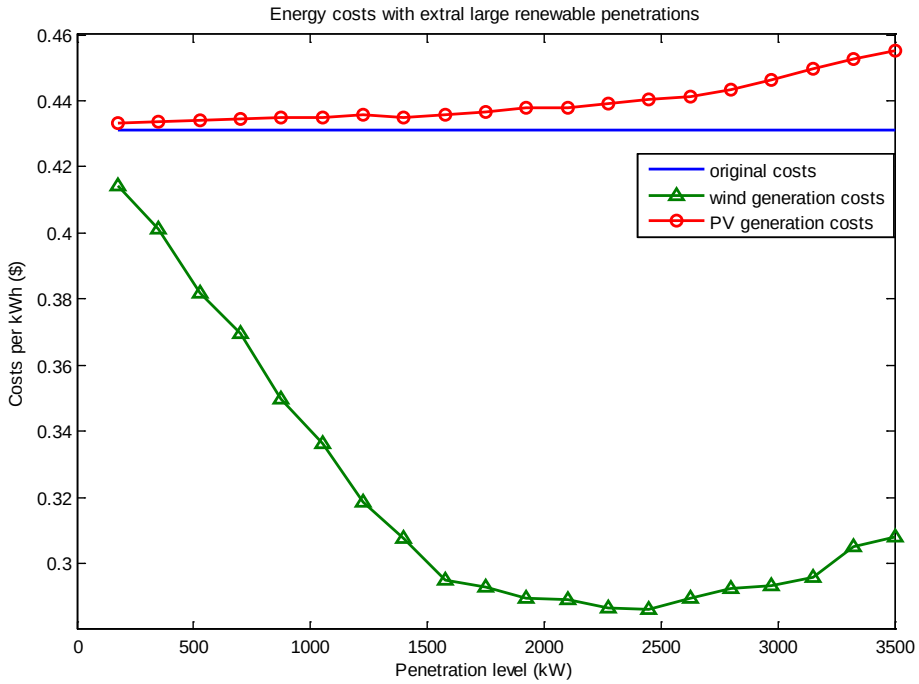

Fig. 5-17 Energy costs with extra high renewable penetration.

Shown from Fig. 5-17 PV generation costs are still higher than diesel generation. The best penetration level of wind is about 2500 kW which will give the lowest energy cost. But this level is much higher than the security limit (1050 kW) which may, as mentioned before, cause serious fluctuations. It is expected that detail modeling of storage units or novel device can help damp the fluctuations and enlarge the limit to 2500 kW level.

6. Conclusions and Future Works

6.1. Conclusions

This thesis focuses on solving the high energy costs of diesel generation in remote isolated areas with renewable penetration. Coober Pedy, a remote town in South Australia, is chosen as an example place to study. The stochastic generation modeling and planning are implemented and the following conclusions can be made.

- To properly describe characteristics of renewable sources, a stochastic model is needed. Random distribution functions are used in this study. The K-S test shows that the Weibull distribution is the best distribution function to fit solar irradiation and wind speed histogram data.

  For some seasons, like spring and fall, histograms of renewable sources may not be unimodal. In these cases the Weibull distribution cannot be accepted by the K-S test. A new bimodal distribution function is generated in the thesis and the results show good fit.

- Generation fluctuation is a problem of renewable generation. Storage unit and power limiter are common methods to deal with such problems. Evaluations of storage unit and power limiter are made in Chapter 4 which, however, reveal that the costs of a storage unit is prohibitive and the power limiters will seriously lower the efficiency of renewable generation. The original diesel generators are set as backup power to renewable generations.

- Sequential Monte Carlo simulation is used to perform the planning study. Planning renewable generation focuses on energy sufficiency and costs. A certain

amount of diesel generators are excluded to lower the energy costs. Simulation shows PV generation is more expensive than diesel generation but wind power costs less. When the penetration level gets higher, PV generation costs go higher but wind generation costs go lower. Under a security limit of 30% of total load demand, 350 kW wind power penetration with 1 diesel generator excluded is the optimal choice.

- Some special cases are discussed and tested. It is shown that when wind generation goes extra high, the costs will not monotonically decrease. The maximum penetration level is 2500 kW.
- A larger wind turbine will not lower the energy costs, because in Coober Pedy, the average load is about 1250 kW and the capacity of a large wind turbine usually larger than 1 MW. In other words, the capacity factor of the large wind turbine is less than 12.5%. The low capacity factor raises the energy cost of a large wind turbine.

6.2. Future works

The results of Coober Pedy provide a reference to the places which have a similar environment. The results given in this study show a rough estimation of costs and penetration level of renewable energy. There are still some topics that can be studied in future.

- In this study, the grid in Coober Pedy is assumed to be one wire. However, in reality the grid structure maybe more complex. Moreover, in regions around

Coober Pedy there are some other isolated micro grids, whether these isolated micro grid can be interconnected is a new topic to study.

- With the grid structure mentioned above, the security limit can be studied and verified with the 30% standard claimed by the local government.
- In Chapter 4, storage units are discussed. A rough evaluation of storage unit size and costs is made. The accuracy of this evaluation is limited by the lack of model of storage units. It will be beneficial if a detailed model of the storage unit and its connection to the grid is modeled.
- In this study, the stochastic models of renewable sources are built based on distribution functions. There is a disadvantage of this method that in every time spot the value of wind speed or solar irradiation is uncorrelated. As a result high frequency and dramatic fluctuations are generated. These problems will enlarge the estimated storage unit sizes. As introduced in Chapter 2, random process is an alternative method to solve such problems.
- The maintenance of the renewable device and diesel generators is not considered in reliability analysis. It will be helpful this factor is considered and a Unit Commitment (UC) schedule can be developed which will help ensure energy sufficiency and also protect the diesel generators from frequent switching behaviors.

References

[1] KPMG, “Remote Areas Energy Supply Scheme Final Report”, Department of Transport & Infrastructure-Energy Division, Australia, June 2011.

[2] M. Nick, G.H. Riahy, S.H. Hosseinian, F. Fallahi, "Wind power optimal capacity allocation to remote areas taking into account transmission connection requirements," *IET Renewable Power Generation*, vol. 5, no. 5, pp. 347-355, Sep 2011.

[3] J.A.M. Bleijs, "Wind turbine dynamic response--difference between connection to large utility network and isolated diesel micro-grid," *Renewable Power Generation, IET*, vol. 1, no. 2, pp. 95-106, June 2007.

[4] R. Billinton, R. Karki, "Capacity expansion of small isolated power systems using PV and wind energy," *IEEE Transactions on Power Systems*, vol. 16, no. 4, pp. 892-897, Nov 2001.

[5] NREL (2010, July). *Supporting Data for Energy Technology Costs, re_costs_20100618.xls*, [online]. Available: http://www.nrel.gov/analysis/tech_cost_dg.html

[6] S. Virinder, “Blending wind and solar into the diesel generator market”, Renewable Energy Policy Project, Washington, Rep. No. 12, 2001.

[7] EIA (2012, May 21). *Weekly U.S. No.2 Diesel Retail Prices (Dollars per Gallon) EMD_EPD2D_PTE_NUS_DPGw.xls* [online]. Available: http://tonto.eia.gov/dnav/pet/hist/LeafHandler.ashx?n=PET&s=EMD_EPD2D_PTE_NUS_DPG&f=W

[8] V. N. Chemmangot, “High Renewable Energy Penetration Diesel Generator System,” *Path to sustainable energy*, Shanghai, China: InTech, 2010, ch. 25, pp. 511-536.

[9] F. Nadeye *et al*, “Remote Area Power Supply (RAPS) Load and Resource Profile”, Sandia National Laboratory, Albuquerque, NM, Rep. SAND2007-4268, 2007.

[10] J.M. Carrasco *et al*, “Power-Electronic Systems for the Grid Integration of Renewable Energy Sources: A Survey,” *IEEE Transactions on Industrial Electronics*, vol. 53, no. 4, pp. 1002-1016, June 2006.

[11] S.J. Irazimi, M. Fathi, “Analysis of hybrid Wind/Fuel cell /Battery/ diesel energy system under Alaska condition,” *Electrical Engineering/Electronics, Computer, Telecommunications and Information Technology (ECTI-CON), 2011 8th International Conference on*, pp. 917-920, 17-19 May 2011.

[12] D. Curtis, B.N. Singh. (2010). *Northern micro-grid project-a concept,* [online]. Available: http://www.worldenergy.org/documents/congresspapers/395.pdf

[13] A. A. Setiawan, C. V. Nayar. (2006). *Design of hybrid power system for a island in Maldive,* [online]. Available: http://www.homerenergy.com/webcast-downloads/Webcast_HOMER-Ahmad.pdf

[14] Johnson, L. Gary, "Economic Design of Wind Electric Systems," *IEEE Transactions on Power Apparatus and Systems,* vol. PAS-97, no. 2, pp. 554-562, March 1978.

[15] T. A. Rauh, W. Seelert, "The Betz optimum efficiency for windmills," *Applied Energy,* vol. 17, Issue 1, pp. 15-23, 1984.

[16] A.A. Chowdhury, "Reliability models for large wind farms in generation system planning," *IEEE Power Engineering Society General Meeting*, vol. 2, pp. 1926-1933, June 2005.

[17] Z.M. Salameh, B.S. Borowy, A.R.A. Amin, "Photovoltaic module-site matching based on the capacity factors," *IEEE Transactions on Energy Conversion*, vol. 10, no. 2, pp. 326-332, Jun 1995.

[18] Md.H. Rahman, S. Yamashiro, "Novel Distributed Power Generating System of PV-ECaSS Using Solar Energy Estimation," *IEEE Transactions on Energy Conversion*, vol. 22, no. 2, pp. 358-367, June 2007.

[19] J.V. Seguro, T.W. Lambert, "Modern estimation of the parameters of the Weibull wind speed distribution for wind energy analysis", *Journal of Wind Engineering and Industrial Aerodynamics,* vol. 85, Issue 1, pp. 75-84, March 2000.

[20] I. Abouzahr, R. Ramakumar, "An approach to assess the performance of utility-interactive wind electric conversion systems," *IEEE Transactions on Energy Conversion,* vol. 6, no. 4, pp. 627-638, Dec 1991.

[21] Y.M. Atwa, E.F. El-Saadany, M.M.A. Salama, R. Seethapathy, "Optimal Renewable Resources Mix for Distribution System Energy Loss Minimization," *IEEE Transactions on Power Systems,* vol. 25, no. 1, pp. 360-370, Feb. 2010.

[22] J. Hetzer, D.C. Yu, K. Bhattarai, "An Economic Dispatch Model Incorporating Wind Power," *IEEE Transactions on Energy Conversion,* vol. 23, no. 2, pp. 603-611, June 2008.

[23] R. Karki, Hu Po, R. Billinton, "A simplified wind power generation model for reliability evaluation," *IEEE Transactions on Energy Conversion*, vol. 21, no. 2, pp. 533- 540, June 2006.

[24] R. Karki, Hu Po, "Wind power simulation model for reliability evaluation," *Canadian Conference on Electrical and Computer Engineering 2005*, pp. 541-544, 1-4 May 2005.

[25] S. Wang, M.E. Baran, "Reliability assessment of power systems with wind power generation," *2010 IEEE Power and Energy Society General Meeting*, pp. 1-8, 25-29 July 2010.

[26] Y.M. Atwa, E.F. El-Saadany, "Optimal Allocation of ESS in Distribution Systems With a High Penetration of Wind Energy," *IEEE Transactions on Power Systems*, vol. 25, no. 4, pp. 1815-1822, Nov. 2010.

[27] H. Nikkhajoei, M.R. Iravani, "A matrix converter based micro-turbine distributed generation system," *IEEE Transactions on Power Delivery*, vol. 20, no. 3, pp. 2182- 2192, July 2005.

[28] S.A. Daniel, N. Ammasai Gounden, "A novel hybrid isolated generating system based on PV fed inverter-assisted wind-driven induction Generators," *IEEE Transactions on Energy Conversion*, vol. 19, no. 2, pp. 416- 422, June 2004.

[29] T. Senjyu, T. Nakaji, K. Uezato, T. Funabashi, "A hybrid power system using alternative energy facilities in isolated island," *IEEE Transactions on Energy Conversion*, vol. 20, no. 2, pp. 406-414, June 2005.

[30] F.A. Bhuiyan, A. Yazdani, "Multimode Control of a DFIG-Based Wind-Power Unit for Remote Applications," *IEEE Transactions on Power Delivery*, vol. 24, no. 4, pp. 2079-2089, Oct. 2009.

[31] M. Datta, T. Senjyu, A. Yona, T. Funabashi, Kim Chul-Hwan, "A Coordinated Control Method for Leveling PV Output Power Fluctuations of PV–Diesel Hybrid Systems Connected to Isolated Power Utility," *IEEE Transactions on Energy Conversion*, vol. 24, no. 1, pp. 153-162, March 2009.

[32] Department of Climate Change and Energy Efficiency of Australia, “SA Wind Energy Program 1984-1989 Data Files”, unpublished data, email communication with J. Nickolas, Nov. 2011.

[33] R. Bento, P. Martinho, C. G. Soares, "Modelling wave energy resources for UK's southwest coast," *OCEANS, 2011 IEEE – Spain*, pp. 1-8, 6-9 June 2011.

[34] P. Sorensen, N. A. Cutululis, A. Vigueras-Rodriguez, L. E. Jensen, J. Hjerrild, M. H. Donovan, H. Madsen, "Power Fluctuations From Large Wind Farms," *IEEE Transactions on Power Systems*, vol. 22, no. 3, pp. 958-965, Aug. 2007.

[35] Lu Ming-Shun, Chang Chung-Liang, Lee Wei-Jen, Wang Li, "Combining the Wind Power Generation System With Energy Storage Equipment," *IEEE Transactions on Industry Applications*, vol. 45, no. 6, pp. 2109-2115, Nov.-Dec. 2009.

[36] M. Datta, T. Senjyu, A. Yona, T. Funabashi, Kim Chul-Hwan, "A Coordinated Control Method for Leveling PV Output Power Fluctuations of PV–Diesel Hybrid Systems Connected to Isolated Power Utility," *IEEE Transactions on Energy Conversion*, vol. 24, no. 1, pp. 153-162, March 2009.

[37] J. R. Kristoffersen, "The HORNS REV wind farm and the operational experiencewith the wind farm main controller," *Copenhagen Offshore Wind 2005*, 26-28, pp. 1-9, Oct. 2005.

[38] D. Paul, E. Erik, K. Brendan, M. Michael, "The role of energy storage with renewable electricity generation," NREL, Golden, CO, Rep. NREL/TP-6A2-47187, 2011.

[39] Arulampalam, M. Barnes, N. Jenkins, J.B. Ekanayake, "Power quality and stability improvement of a wind farm using STATCOM supported with hybrid battery energy storage," *IEE Proceedings on Generation, Transmission and Distribution*, vol. 153, no. 6, pp. 701-710, Nov. 2006.

[40] P.Ahmad, S. Kandler, M. Tony, "Impact of the 3Cs of Batteries on PHEV Value Proposition: Cost, Calendar Life, and Cycle Life," NREL, Golden, CO, Rep. NREL/PR-540-45887, 2009.

[41] J. F. Lee, "Optimization of Utility-Scale Wind-Hydrogen-Battery Systems," NREL, Denver, CO, Rep. NREL/CP-500-36117, 2004.

[42] M. S. Susan, V. H. William, Long- vs. Short-Term Energy Storage Technologies Analysis, Sandia National Laboratries, Albuquerque, NM, Rep. SAND2003-2783, 2003.

[43] K. E. Holbert, D. Srinivasan, "Solar Energy Calculations," *Handbook of Renewable Energy Technology*, edited by A. F. Zobaa and R. C. Bansal, World Scientific Publishing Co., 2011, Chapter 8, pp. 189-204.

[44] L. Fingersh, M. Hand, A. Laxson, Wind turbine design cost and scaling model, NREL, Golden, CO, Rep. NREL/TP-500-40566, 2006.

[45] Department of Energy. (Aug. 2011). *Small wind economic model* _wind_economic_model.xls, [online], available at:

http://www.windpoweringamerica.gov/docs/small_wind_economic_model.xls.

[46] Levelized costs of new generation resources in annual energy outlook 2011, EIA, Rep. DOE/EIA-0383(2010), 2011.

APPENDIX A
NORMALIZATION FACTOR FOR WIND SPEED AND SOLAR RADIATION

Table 1 Normalization factor for solar radiation

	Solar radiation level (W/m^2)												
Time	6:00	7:00	8:00	9:00	10:00	11:00	12:00	13:00	14:00	15:00	16:00	17:00	18:00
Spring	176	312	594	782	924	953	1029	1129	1118	1100	835	624	676
Summer	560	630	820	1300	1410	1428	1521	1024	959	929	829	741	135
Fall	141	141	347	565	682	794	835	794	765	647	506	318	235
Winter	247	253	247	271	376	612	576	529	494	400	241	224	306

Table 2 Normalization factor for wind speed (from 1:00 to 12:00)

	Wind speed (m/s)											
Time	1:00	2:00	3:00	4:00	5:00	6:00	7:00	8:00	9:00	10:00	11:00	12:00
Spring	23.27	30.09	24.26	23.27	25.69	23.27	22.7	25.83	29.8	25.31	27.96	29.66
Summer	20.71	32.51	35.62	25.98	25.54	27.11	28.38	29.09	28.67	34.92	35.62	36.62
Fall	25.54	24.97	25.69	24.41	30.79	24.83	29.09	25.54	26.97	25.98	34.06	26.11
Winter	27.68	25.69	26.68	25.98	25.98	23.98	26.82	30.22	26.11	25.83	25.4	27.81

Table 3 Normalization factor for wind speed (from 13:00 to 24:00)

	Wind speed (m/s)											
Time	13:00	14:00	15:00	16:00	17:00	18:00	19:00	20:00	21:00	22:00	23:00	24:00
Spring	28.38	28.34	28.06	25.69	25.98	26.11	28.96	25.98	27.96	29.23	23.69	28.38
Summer	31.08	28.52	26.11	24.26	25.26	34.78	21.05	23.98	26.68	19.95	19.4	31.08
Fall	24.55	25.69	27.53	26.68	26.25	27.24	27.68	23.13	22.99	23.42	21.99	24.55
Winter	26.54	26.68	26.25	28.1	27.68	27.39	29.3	25.69	29.8	31.36	29.23	26.54